No. 2038

TECHNICAL REPORT

DECAY OF A DISCONTINUITY LINE IN A VISCOUS FLUID

by

Hans J. Lugt

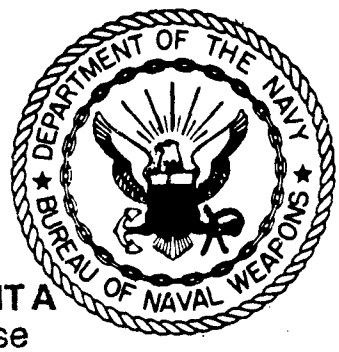

U. S. NAVAL WEAPONS LABORATORY
DAHLGREN, VIRGINIA

U. S. Naval Weapons Laboratory
Dahlgren, Virginia

Decay of a Discontinuity Line in a Viscous Fluid

by

Hans J. Lugt
Computation and Analysis Laboratory

NWL REPORT NO. 2038

Task Assignment
NO. R360FR103/2101/R0110101

May 1966

TABLE OF CONTENTS

ABSTRACT

Integral transforms are used to solve singular initial value problems for Stokes' slow-motion equations. The method is applied to investigate the decaying process of straight and circular discontinuity lines as well as the dissipation of local disturbances in an infinite medium. A criterion for the occurrence of secondary vortices is derived. Numerical results are displayed for periodic initial disturbances which demonstrate graphically the spreading of the disturbance from a discontinuity line into the fluid under successive development and decay of secondary vortices. A more detailed sequence of dissipating vortices is evaluated numerically and displayed by streamline patterns in connection with Lamb's vortical eigenmotions in an infinitely long cylinder of finite radius.

FOREWORD

This work was sponsored by the Foundational Research Program of the U. S. Naval Weapons Laboratory under the technical direction of Mr. B. Smith. It was performed in the Computation and Analysis Laboratory as part of the project, Mathematical Theory of Viscous Flow (R360FR103/2101/R0110101). The author would like to thank Dr. E. W. Schwiderski for many fruitful discussions and comments. The author also extends his thanks to Messrs. R. L. Fausey and E. Pool for their programming.

Part of this paper was presented at the Symposium of the International Union of Theoretical and Applied Mechanics on Rotating Fluid Systems in La Jolla, California, 28 March - 2 April, 1966.

The date of completion was May 12, 1966.

Approved for Release:

/s/ BERNARD SMITH
Technical Director

1. Introduction

In a recent paper [1] complete systems of time-dependent separable solutions of Stokes' slow-motion equations have been constructed for rectangular and annular flow regions. This was achieved by means of a generalized separation technique introduced in [2, 3]. In addition, so-called associated separable solutions have been found by differentiating or integrating separable solutions with respect to an integration parameter. Their significance for the construction of certain solutions of the complete Navier-Stokes equations has been pointed out.

With the aid of those separable solutions eigenmotions have been determined which are required to satisfy certain incomplete boundary data without prescribed initial values. For given boundary and initial data a discrete or continuous superposition of eigenmotions is necessary. Because of the complicated nature of this fitting procedure the introduction of integral transforms suggests itself. They can be utilized because separable solutions exist.

In this paper the integral transform technique is applied to describe decaying straight and coaxial discontinuity lines as well as the obliteration of local disturbances in a laminar fluid flow. The analysis is restricted to plane motions so that use can be made of the stream function ψ. Hence, Stokes' slow-motion equations are reduced to the single fourth order partial differential equation

$$\left(\Delta - \frac{\partial}{\partial t}\right)\Delta\psi = 0 \qquad (1)$$

where Δ is the Laplacian operator and t the product of time and constant kinematic viscosity. Numerical results are obtained for selected examples which demonstrate graphically the sequence of decay.

It may be mentioned that under certain boundary and regularity conditions the solutions obtained can be used to derive integrals of the quasi-linear Navier-Stokes equations in an exact linear manner by an iterative procedure. This has been shown in [1, 2, 3] for various flow problems.

2. Decay of a Straight Discontinuity Line in an Infinite Region

A straight discontinuity line may be generated by two uniform parallel flows of opposite direction at $t = 0$ and may be located at the axis $y = 0$ in a Cartesian coordinate system (x, y). (Fig. 1). In addition, a disturbance along the discontinuity line is superposed which may be of periodic or aperiodic nature expressed by a Fourier series or Fourier integral, respectively. Hence, a slow-motion solution of Stokes' equation (1) in Cartesian coordinates

$$\psi_{xxxx} + 2\psi_{xxyy} + \psi_{yyyy} = (\psi_{xx} + \psi_{yy})_t \qquad (2)$$

may be specified by the following initial and boundary conditions. The initial state is described by the basic flow

$$\psi_B(x, y, 0) = A_B |y| \quad , \qquad (A_B \geq 0) \qquad (3)$$

and the disturbance

$$\psi(x, y, 0) = \begin{cases} \delta(y) \sum_{n=-\infty}^{+\infty} A(n) e^{inx} \\ \delta(y) \int_{-\infty}^{+\infty} A(n) e^{inx} dn \end{cases} . \tag{4}$$

The discrete or continuous function A(n) is assumed to yield convergence of the series or integral, respectively. Furthermore, $A(-n) = \bar{A}(n)$, where $\bar{A}$ is the conjugate complex value of A. The symbol $\delta(y)$ denotes Dirac's delta function. The boundary conditions for $t \geq 0$ and $-\infty \leq x \leq +\infty$ are

$$y = \pm \infty: \lim_{|y| \to \infty} \frac{\psi_B}{|y|} = A_B \quad , \qquad (\psi_B)_y = \pm A_B \quad , \tag{5}$$

$$\psi = 0 \quad , \qquad \psi_y = 0 \quad . \tag{6}$$

In addition to the conditions (5) and (6) it is required that ψ_B and ψ have a sufficiently monotonic behavior for large values of y. For the x-direction it is assumed that ψ_B and ψ are representable in the forms

$$\psi_B(x, y, t) = S_B(y, t) \tag{7}$$

$$\psi(x, y, t) = \begin{cases} \sum_{n=-\infty}^{+\infty} S(y, t, n) e^{inx} \\ \int_{-\infty}^{+\infty} S(y, t, n) e^{inx} dn \end{cases} \tag{8}$$

with $S(-n) = \bar{S}(n)$. For the sake of simplicity it may be required that the representations of ψ by equation (8) are four times differentiable in space and once in time under the summation or integral symbol. At this point it may be mentioned that this assumption restricts the manifold of solutions considerably. For instance, if general boundary data were imposed at some lines $x = x_0$ and $x = x_1$, it is easy to show through a finite Fourier transformation of equation (2) that the equation (11) below for $S(y, t, n)$ must be augmented by appropriate inhomogeneous terms. A detailed examination of this deficiency of separable solutions will be made in a forthcoming paper by Schwiderski [4].

The initial and boundary data (3) through (8) form together with equation (2) a well-set initial value problem. For the basic flow (3), (5), and (7) the solution

$$\psi_B = \frac{2A_B}{\sqrt{\pi}} \sqrt{t}\left[\frac{y}{2\sqrt{t}} \int_0^{y/2\sqrt{t}} s^{-\frac{1}{2}} e^{-s} ds + e^{-\frac{y^2}{4t}} - 1\right] \tag{9}$$

with the velocity components

$$u_B = (\psi_B)_y = A_B \operatorname{erf}\left(\frac{y}{2\sqrt{t}}\right) , \qquad v_B = -(\psi_B)_x \equiv 0 \tag{10}$$

is well known in literature [5] and is set aside for the time being. The remaining initial value problem for ψ can be solved in the following way:

Insertion of the expansions (8) in equation (2) yields for $S(y, t, n)$ the fourth order differential equation

$$S_{yyyy} - \left(2n^2 + \frac{\partial}{\partial t}\right)S_{yy} + n^2\left(n^2 + \frac{\partial}{\partial t}\right)S = 0 \quad . \tag{11}$$

By introducing the Laplace transform

$$\Phi(y, \lambda^2 - n^2) = \int_0^\infty S(y, t, n)e^{-(\lambda^2-n^2)t}dt \tag{12}$$

one arrives for equation (11) at

$$\left(\frac{\partial^2}{\partial y^2} - n^2\right)\left(\frac{\partial^2}{\partial y^2} - \lambda^2\right)\Phi = - \left(\frac{\partial^2}{\partial y^2} - n^2\right)S(y, 0, n) \quad , \tag{13}$$

where the initial value $S(y, 0, n) = A(n)\delta(y)$. Equation (13) can be integrated twice to yield the second order differential equation

$$\left(\frac{\partial^2}{\partial y^2} - \lambda^2\right)\Phi = \begin{cases} - A(n)\delta(y) + c_n e^{ny} + d_n e^{-ny}, & n \neq 0 \\ - A(o)\delta(y) + c_o y + d_o \ , & n = 0 \end{cases} \quad . \tag{14}$$

The coefficients c_n and d_n are determined by the boundary condition $\Phi(\pm\infty, \lambda^2 - n^2) = 0$, which one derives from equations (6) and (12). It follows $c_n = d_n = 0$.

An attempt to integrate equation (14) for the desired particular integral would require a differentiation of equation (12) with respect to y in order to achieve the proper regularity at $y = 0$ for all t. Since the delta function is involved for $t = 0$, such differentiation of equation (12) cannot be carried out under the

integral sign. This difficulty is avoided by applying to equation (14) the Fourier transform

$$f_{n,\lambda}(p) = \int_{-\infty}^{+\infty} \Phi(y, \lambda^2 - n^2) e^{ipy} dy \quad . \tag{15}$$

Then, one obtains

$$f_{n,\lambda}(p) = \frac{A(n)}{\lambda^2 + p^2} \quad . \tag{16}$$

In [6, 7] the original function of $f_{n,\lambda}(p)$ with respect to y is tabulated and becomes

$$\Phi = \frac{A(n)}{2\lambda} e^{-\lambda |y|} \quad . \tag{17}$$

This again is the image function of S and can be inverted to

$$S = \frac{A(n)}{2\sqrt{\pi t}} \exp -\left(n^2 t + \frac{y^2}{4t}\right) \quad . \tag{18}$$

Integral (18) belongs to the class of associated separable solutions which have been found in [1] . Substitution of (18) in (4) renders the solution of the initial value problem (2), (4), (6), and (8):

$$\psi(x, y, t) = \frac{1}{2\sqrt{\pi t}} e^{-\frac{y^2}{4t}} \begin{cases} \sum_{n=-\infty}^{+\infty} A(n) e^{inx - n^2 t} & (19a) \\ \int_{-\infty}^{+\infty} A(n) e^{inx - n^2 t} dn \quad . & (19b) \end{cases}$$

Solution (19a) describes the decay of a periodic disturbance which is confined at $t = 0$ to the single line $y = 0$ and which spreads

with advancing time into the fluid in form of a discrete spectrum of vortical motions. Each mode n consists of 2n vortices in the interval from 0 to 2π. For modes $n > 0$ the dissipation of the motions (19a) is essentially governed by the exponential function $\exp(-n^2 t)$. Since its damping coefficient is n^2, vortices of high order n decay faster than those of low order n. Furthermore, those vortices with largest coefficient A(n) dominate at the beginning and become visible as "secondary vortices." The 2n vortices of this dominating mode grow in their spatial extent and die away as soon as they are overcome by vortices of lower modes. This mechanism explains the observed occurrence of small vortices of large number in the beginning of the decaying process of a discontinuity line and their replacement by fewer vortices at a later time (see the experiments by Weske and Rankin [8]).

The process described above may be illustrated by a series of flow patterns at various times. In Figs. 2 through 13 computer output is displayed for streamlines which differ from each other by an equal amount. For convenience the Fourier coefficients A(n) may be expressed by the amplitude C_n and the phase angle α_n such that $A(n) = C_n e^{i\alpha n}$. In the first sequence of figures the motion consists of the superposed modes $n = 1$ and $n = 2$. The ratio of their amplitudes is $C_2 : C_1 = 10$ so that the four vortices of $n = 2$ dominate at the beginning (Fig. 2). Furthermore, the phase angles

of the two modes may differ by $\pi/4$. If time passes by, the second vortex diminishes and its two neighboring vortices join each other, whereas the fourth vortex gains considerable strength (Figs. 3 through 6). The remaining two vortices, then, approach the state which is represented by n = 1 (Fig. 7) and finally die away when t tends to infinity. The same vortex configuration but with equal phase angles ($C_2 : C_1 = 10$, $\alpha_2 - \alpha_1 = 0$) dissolves in a symmetric way by supporting and suppressing two adjacent vortices each (Figs. 8 and 9). In a third sequence of figures a disturbance of mode n = 2 is superposed on the basic flow (9) with $C_2 : A_B = 5\sqrt{\pi}$ and $\alpha_2 = \pi/2$. Fig. 10 shows the flow field in an early stage. With progressing time those vortices are weakened which have flow directions opposite to the main stream (Fig. 11). They finally vanish (Fig. 12), and the remaining two vortices are gradually absorbed by the basic motion (Fig. 13).

From solution (19a) one can derive the criterion for the generation of any secondary vortex which accompanies a dissipating discontinuity line: There must exist at least one mode $n \neq 0$ with nonvanishing A(n) which is sufficiently strong in comparison with $A(\bar{o})$ and A_B.

It may be noted that the solution (19a) exhibits the same decaying mechanism as a complete solution of the Navier-Stokes equations.

As was shown in [1] for the similar case of Lamb's eigenmotions (see section 4), the solutions of Stokes' and Navier-Stokes' equations approach each other during the final phase of decay and become equal if n = 0 prevails.

The decay of an aperiodic disturbance may be illustrated by the example

$$A(n) \equiv 1, \quad \int_{-\infty}^{+\infty} e^{inx} dn = 2\pi \delta(x) \quad . \tag{20}$$

Then, the evaluation of the Fourier integral in (19b) yields the solution

$$\psi = \frac{1}{2t} \exp - \frac{1}{4t}(x^2 + y^2) \quad . \tag{21}$$

Equation (21) describes the decay of a single vortex, where the stream function ψ depends only on the radial distance $r = (x^2 + y^2)^{\frac{1}{2}}$ from the center of the disturbance. This leads to the study of disturbances in a polar coordinate system, which will be the subject of the next section.

3. Decay of a Coaxial Discontinuity Line in an Infinite Region

In literature the solution of a decaying coaxial discontinuity line seems not to be known which is produced by a jump in the angular velocity of a fluid rotating like a solid body. This problem corresponds to that of equation (3) for two parallel flows of opposite direction and is not considered here. Rather the

investigation is focused on disturbances as in the previous section. Different from equation (4) univalent disturbances of a coaxial discontinuity line can only be of periodic nature. Therefore, if r = a designates the location of the singular line, the disturbance is assumed to be of the general form

$$\psi(r, \varphi, 0) = \delta(r - a) \sum_{n=o}^{\infty} A_n \cos(n\varphi + \alpha_n) \quad . \tag{22}$$

For all $t \geq 0$, the disturbance shall vanish at $r = \infty$, that is

$$r = \infty : \qquad \psi = 0 \ , \quad \psi_r = 0 \quad . \tag{23}$$

The solution can be sought as

$$\psi(r, \varphi, t) = \sum_{n=o}^{\infty} G_n(r, t) \cos(n\varphi + \alpha_n) \quad , \tag{24}$$

which reduces Stokes' slow-motion equation (1) in polar coordinates (r, φ) to

$$\left(\frac{\partial^2}{\partial r^2} + \frac{1}{r}\frac{\partial}{\partial r} - \frac{n^2}{r^2}\right)\left(\frac{\partial^2}{\partial r^2} + \frac{1}{r}\frac{\partial}{\partial r} - \frac{n^2}{r^2} - \frac{\partial}{\partial t}\right)G_n = 0 \tag{25}$$

(see [1]). Introducing the Laplace transform

$$\Phi_n(r, \lambda^2) = \int_o^{\infty} G_n(r, t) e^{-\lambda^2 t} dt \tag{26}$$

one arrives at

$$\left(\frac{\partial^2}{\partial r^2} + \frac{1}{r}\frac{\partial}{\partial r} - \frac{n^2}{r^2}\right)\left(\frac{\partial^2}{\partial r^2} + \frac{1}{r}\frac{\partial}{\partial r} - \frac{n^2}{r^2} - \lambda^2\right)\Phi_n = -\left(\frac{\partial^2}{\partial r^2} + \frac{1}{r}\frac{\partial}{\partial r} - \frac{n^2}{r^2}\right)G_n(r,0) \tag{27}$$

where $G_n(r, 0) = A_n\delta(r - a)$. Double integration of (27) yields the second order differential equation

$$\left(\frac{\partial^2}{\partial r^2} + \frac{1}{r}\frac{\partial}{\partial r} - \frac{n^2}{r^2} - \lambda^2\right)\Phi_n = \left\{\begin{array}{ll} -A_n\delta(r-a) + c_n r^n + d_n r^{-n}, & n \neq 0 \\ -A_0\delta(r-a) + c_0 \log r + d_0, & n = 0 \end{array}\right\} . \tag{28}$$

The boundary data (23) and the regularity condition at $r = 0$ require $c_n = d_n = 0$ for $a > 0$. In order to integrate equation (28) the Hankel transform of order n must be applied,

$$h_{n,\lambda}(p) = \int_0^\infty \sqrt{r}\ \Phi_n(r) J_n(rp)\sqrt{rp}\ dr, \qquad p > 0 \ , \tag{29}$$

where J_n is the n^{th} order Bessel function. This transformation leads to

$$(p^2 + \lambda^2)h_{n,\lambda} = A_n \int_0^\infty \sqrt{r}\ \delta(r - a)J_n(rp)\sqrt{rp}\ dr \tag{30}$$

or by evaluating the integral on the right to

$$h_{n,\lambda} = \frac{1}{p^2 + \lambda^2}[A_n a\sqrt{p}\ J_n(ap)] \ , \qquad a > 0 \ . \tag{31}$$

This function is readily inverted with respect to t and yields

$$H_n(p) = A_n a\sqrt{p}\ J_n(ap)e^{-p^2 t} \ . \tag{32}$$

According to [6, Vol. II, p. 51] the original function of $H_n(p)$ is

$$G_n(r, t) = \frac{1}{2t} A_n a I_n\left(\frac{ar}{2t}\right)\exp\left(-\frac{r^2 + a^2}{4t}\right) \tag{33}$$

with I_n as n^{th} order modified Bessel function of first kind. Hence,

$$\psi(r,\varphi,t) = \frac{a}{2t}\exp\left(-\frac{r^2+a^2}{4t}\right)\sum_{n=o}^{\infty} A_n I_n\left(\frac{ar}{2t}\right)\cos(n\varphi + \alpha_n) \quad , \quad a > 0 \quad . \qquad (34)$$

Since the asymptotic behavior of $I_n\left(\frac{ar}{2t}\right) \sim \left(\frac{ar}{2t}\right)^{-\frac{1}{2}} \exp\left(\frac{ar}{2t}\right)$ is independent of n, the initial state (22) and the boundary conditions (23) can easily be verified. The motion which is represented by the integral (34) corresponds to that of (19a) for a straight discontinuity line. Therefore, its description is here omitted.

It may be mentioned that the special case n = 0 of the integral (34) appears in [9] as the vorticity ω of a decaying discontinuity line. Since this solution fulfills the initial condition $\omega(r, \varphi, 0) = \delta(r - a)$, the discontinuity line considered in [9] is of the form

$$u(r, \varphi, 0) \equiv 0, \quad v(r, \varphi, 0) = \left\{ \begin{array}{l} \frac{a}{r} \text{ for } r \geq a \\ \\ 0 \text{ for } r < a \end{array} \right\} ,$$

where $\omega r = (rv)_r$.

A slightly different situation arises for a = 0 if the coaxial discontinuity line degenerates to a local disturbance. Then, the integral to the right of equation (30) is zero. However, if one changes the coefficients in (22) from A_n to $A_n r^{-1-n}$ one arrives at the image function

$$h_{n,\lambda} = \frac{1}{n!} A_n 2^{-n} \frac{p^{n+\frac{1}{2}}}{p^2 + \lambda^2} \quad , \qquad (35)$$

whereby the coefficient d_n in equation (28) must vanish in order to obtain a finite expression for $h_{n,\lambda}$. According to [6, Vol. II, p. 63] the inversion of (35) with respect to r results in

$$\Phi_n = \frac{1}{n!} A_n 2^{-n} \lambda^n K_n(\lambda r) \quad , \tag{36}$$

where K_n is the n^{th} order modified Bessel function of second kind. Finally, the inverted function of (36) with respect to t is

$$G_n(r,t) = \frac{A_n}{n!} 2^{-n} \frac{r^n}{(2t)^{n+1}} e^{-\frac{r^2}{4t}} \quad , \tag{37}$$

(see [7, p. 128]). Formally, the integral (37) can be obtained from (33) if one replaces A_n by $A_n a^{-1-n}$ and determines the limit for $a \to 0$.

The integral (37) belongs to the class of associated separable solutions which have been constructed and discussed in [1]. They are interpreted as "explosive rotations." The special case n = 0 may be compared with equation (21). It follows that the initial conditions $\psi(x, y, 0) = 2\pi\delta(x)\delta(y)$ and $\psi(r, y, 0) = \frac{1}{r}\delta(r)$ are equivalent. Indeed, they lead to the same solution.

4. Decay of Vortices in an Infinitely Long Cylinder of Finite Radius

The sequence of decaying vortices from higher modes downward to lower ones, which have been described in section 2 for a straight discontinuity line in an infinite flow region, shall now be demonstrated by means of a vortex configuration in a finite circle,

since this process has much resemblance to the phenomenon observed by Weske and Rankin [8]. The vortices at t = 0 may be considered as an intermediate state of a dissipating discontinuity line. As was pointed out in [1] such a decay can be described by Lamb's eigenfunctions

$$\psi_{mn} = A_{mn}\cos(n\varphi + \alpha_{mn})[J_n(\lambda_{mn}r) - J_n(\lambda_{mn})r^n]\exp(-\lambda_{mn}^2 t) \tag{38}$$

$$J_{n+1}(\lambda_{mn}) = 0 \qquad n = 0, 1, 2 \ldots, \quad m = 1, 2, 3, \ldots \tag{39}$$

where the second equation determines the eigenvalues λ_{mn}, and where the radius of the cylinder is unity.

For numerical calculations a vortex ensemble has been selected that consists of the three modes m = 1; n = 2, 3, 4. They represent 4, 6, and 8 vortices each. The amplitudes are arranged to have the ratios $A_4:A_3:A_2$ = 10,000:1000:1 so that the mode n = 4 dominates at t = 0 over the other two (Fig. 14), and so that n = 3 prevails over n = 2 at a later time. The phase angles are zero. In order to exhibit the essential features in the decaying process the following steps are selected: At t = 0.11 (Fig. 15) the flow field in the lower half of the cylinder has weakened in such a way that the vortex which was near the 180° mark in Fig. 14, does not appear any more, and that the two neighboring vortices are about to join. The latter incidence happens at t = 0.13 (Fig. 16). Six vortices are now visible and regroup until an almost symmetric configuration (that is the prevailing mode n = 3) is reached at t = 0.25 (Fig. 17).

Then, the same process repeats itself and ends with four dominating vortices (Figs. 18 through 21) which dissipate slowly when $t \to \infty$. The asymmetric decay is owing to the property of the trigonometric function and can be observed in the photographs by Weske and Rankin [8].

It may be mentioned that the period of time from one dominating mode to the other can be minimized by selecting optimal values for the amplitudes and phase angles. This time interval increases with lower modes. For the example above the ratio of the time intervals, which are required to expose the vortices of modes $n = 3$ and 2 respectively, is 1:2.2. This compares favorably with Weske and Rankin's observation of 1:2.5 [10].

REFERENCES

[1] Lugt, H. J. and Schwiderski, E. W., Birth and Decay of Vortices, Phys. Fluids 9 (1966), No. 6.

[2] Lugt, H. J. and Schwiderski, E. W., Flows around dihedral angles I. Eigenmotion analysis, Proc. Roy. Soc. A, 285 (1965), 382.

[3] Schwiderski, E. W., Lugt, H. J., and Ugincius, P., Axisymmetric Viscous Fluid Motions Around Conical Surfaces, Journ. SIAM 14 (1966), 191.

[4] Schwiderski, E. W., Private communication.

[5] Lamb, H., Hydrodynamics, Dover Publications, New York, 1945, 6th ed.

[6] Bateman Manuscript Project, Tables of Integral Transforms, McGraw-Hill Book Company, Inc., New York, Toronto, London, 1954.

[7] Magnus, W. and Oberhettinger, F., Formulas and Theorems for the Special Functions of Mathematical Physics, Chelsea Publishing Company, New York, 1949.

[8] Weske, J. R. and Rankin, T. M., On the Generation of Secondary Motions in the Field of a Vortex, Phys. Fluids 6 (1963), 1397.

[9] Müller, W., Einführung in die Theorie der zähen Flüssigkeiten, Akademische Verlagsgesellschaft, m. b. H., Leipzig 1932, p. 115.

[10] Weske, J. R. and Rankin, T. M., Production of Secondary Vortices in the Field of a Primary Vortex, The Institute for Fluid Dynamics and Applied Mathematics, University of Maryland, Technical Note BN-244, AFOSR-623, April 1961.

TABLE OF SYMBOLS

a	radius of the coaxial discontinuity line
$A(n)$	Fourier coefficient
I_n	modified n^{th} order Bessel Function of first kind
J_n	n^{th} order Bessel function of first kind
K_n	modified n^{th} order Bessel function of second kind
(r, φ)	polar coordinate system
t	product of time and kinematic viscosity
(u, v)	velocity corresponding to (x, y) or (r, φ)
(x, y)	Cartesian coordinate system
α_n	phase angle
δ	Dirac's delta function
λ_{mn}	eigenvalues
ψ	stream function
ω	vorticity

APPENDIX A

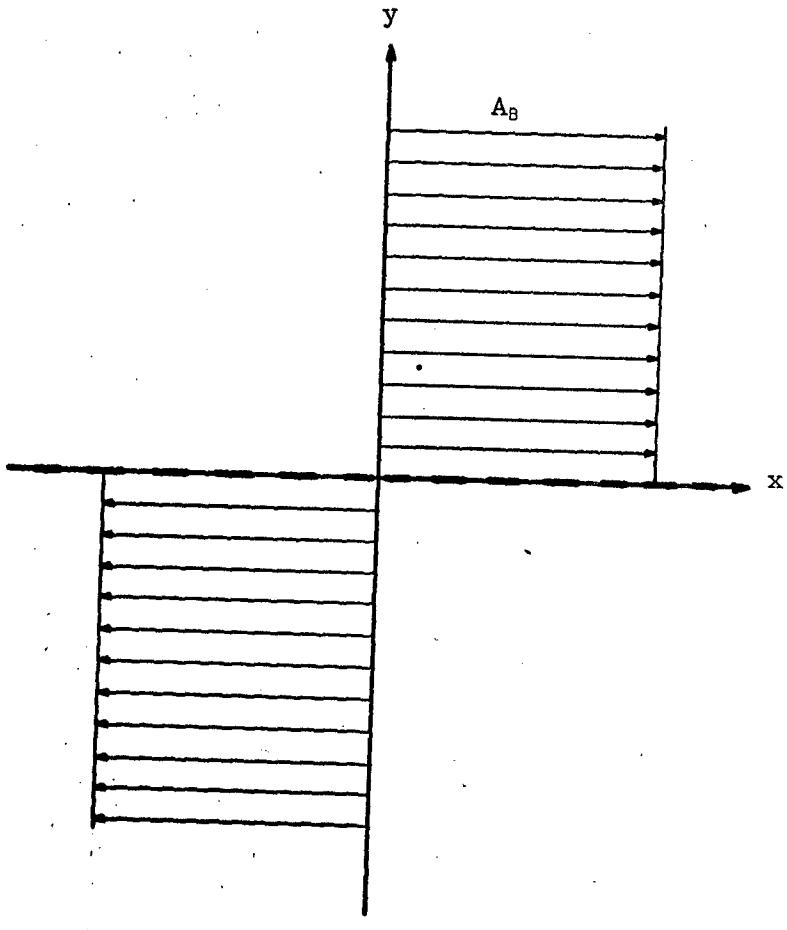

Fig. 1: Sketch of a velocity profile with discontinuity line at y = 0.

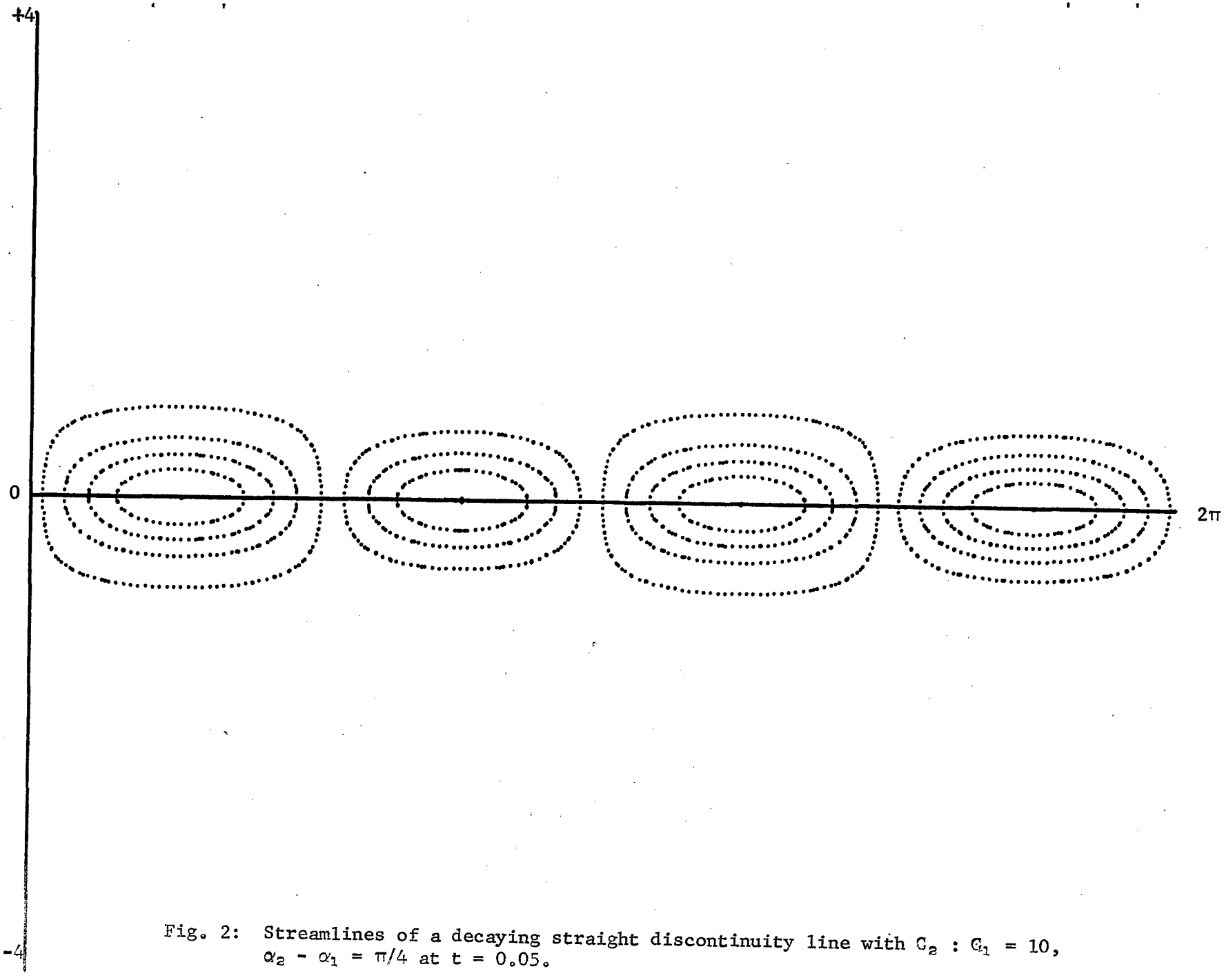

Fig. 2: Streamlines of a decaying straight discontinuity line with $C_2 : C_1 = 10$, $\alpha_2 - \alpha_1 = \pi/4$ at $t = 0.05$.

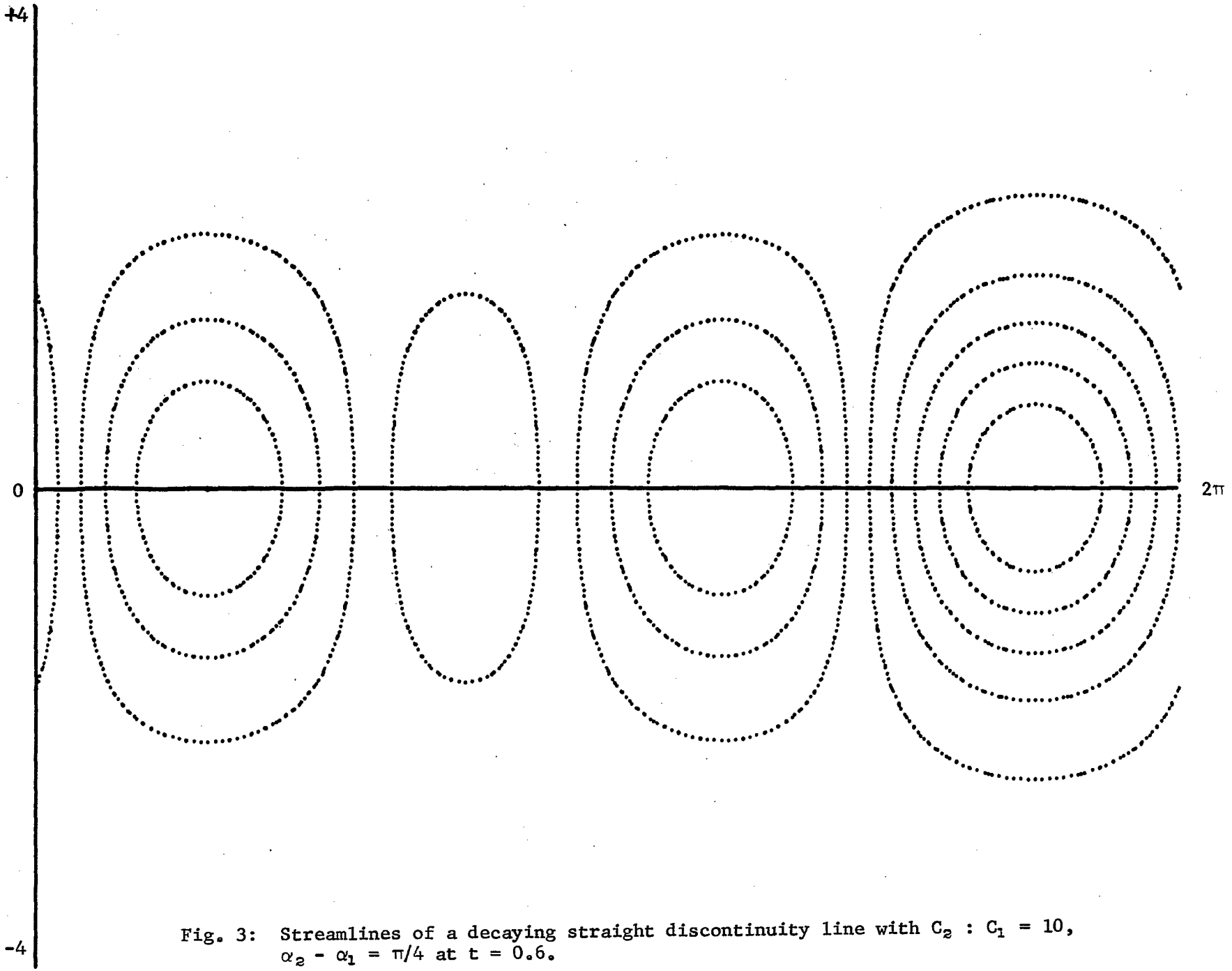

Fig. 3: Streamlines of a decaying straight discontinuity line with $C_2 : C_1 = 10$, $\alpha_2 - \alpha_1 = \pi/4$ at $t = 0.6$.

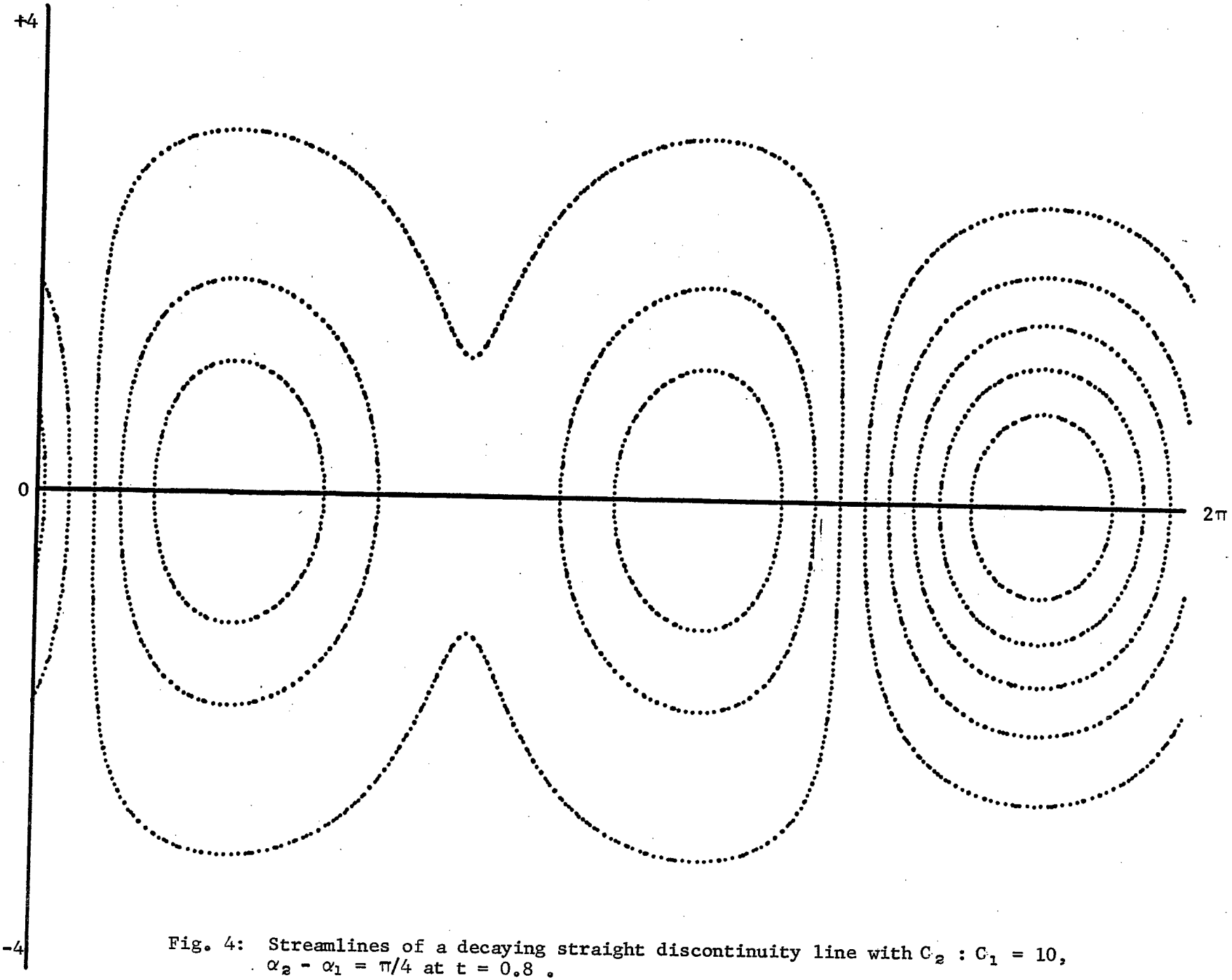

Fig. 4: Streamlines of a decaying straight discontinuity line with $C_2 : C_1 = 10$, $\alpha_2 - \alpha_1 = \pi/4$ at $t = 0.8$.

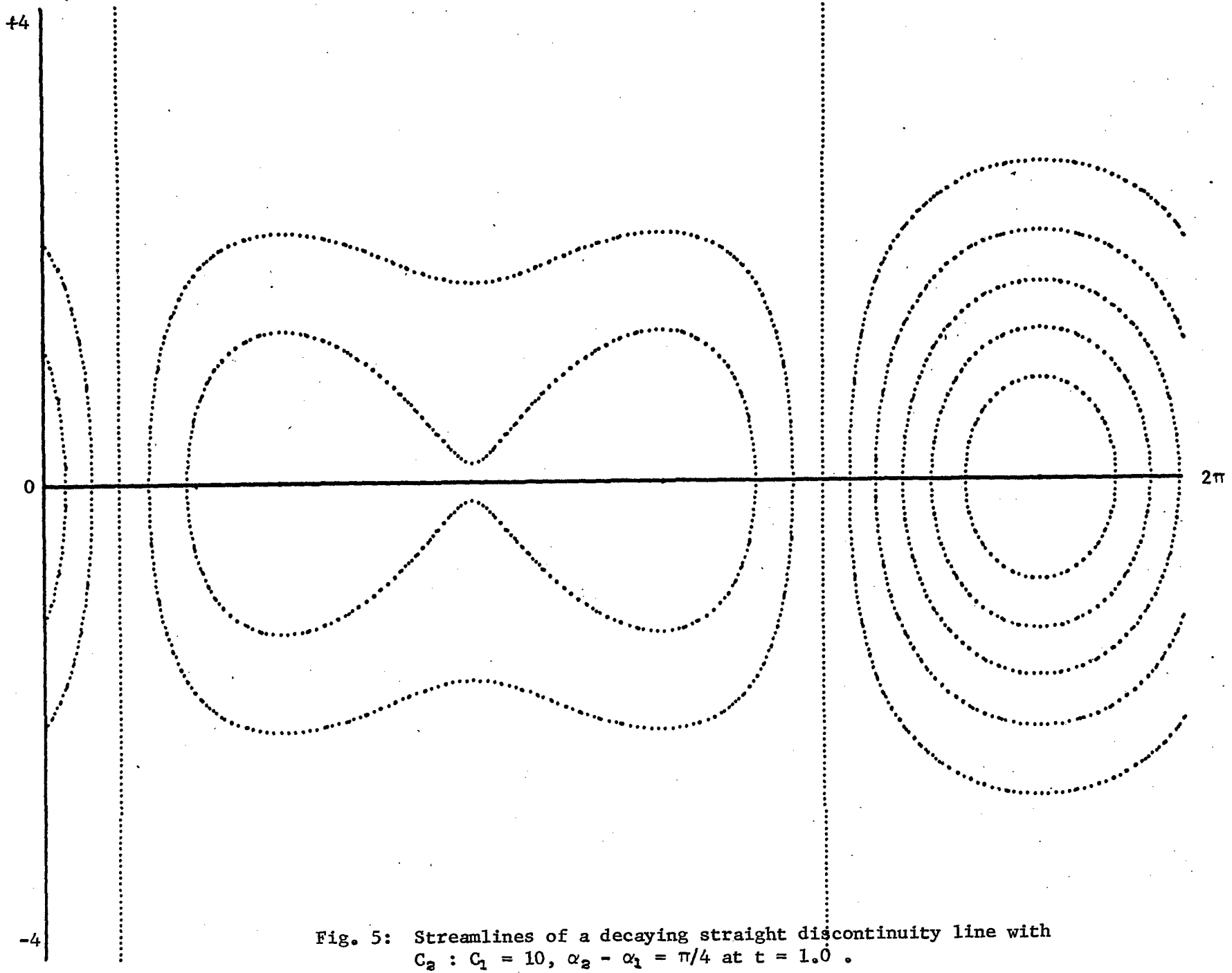

Fig. 5: Streamlines of a decaying straight discontinuity line with $C_2 : C_1 = 10$, $\alpha_2 - \alpha_1 = \pi/4$ at $t = 1.0$.

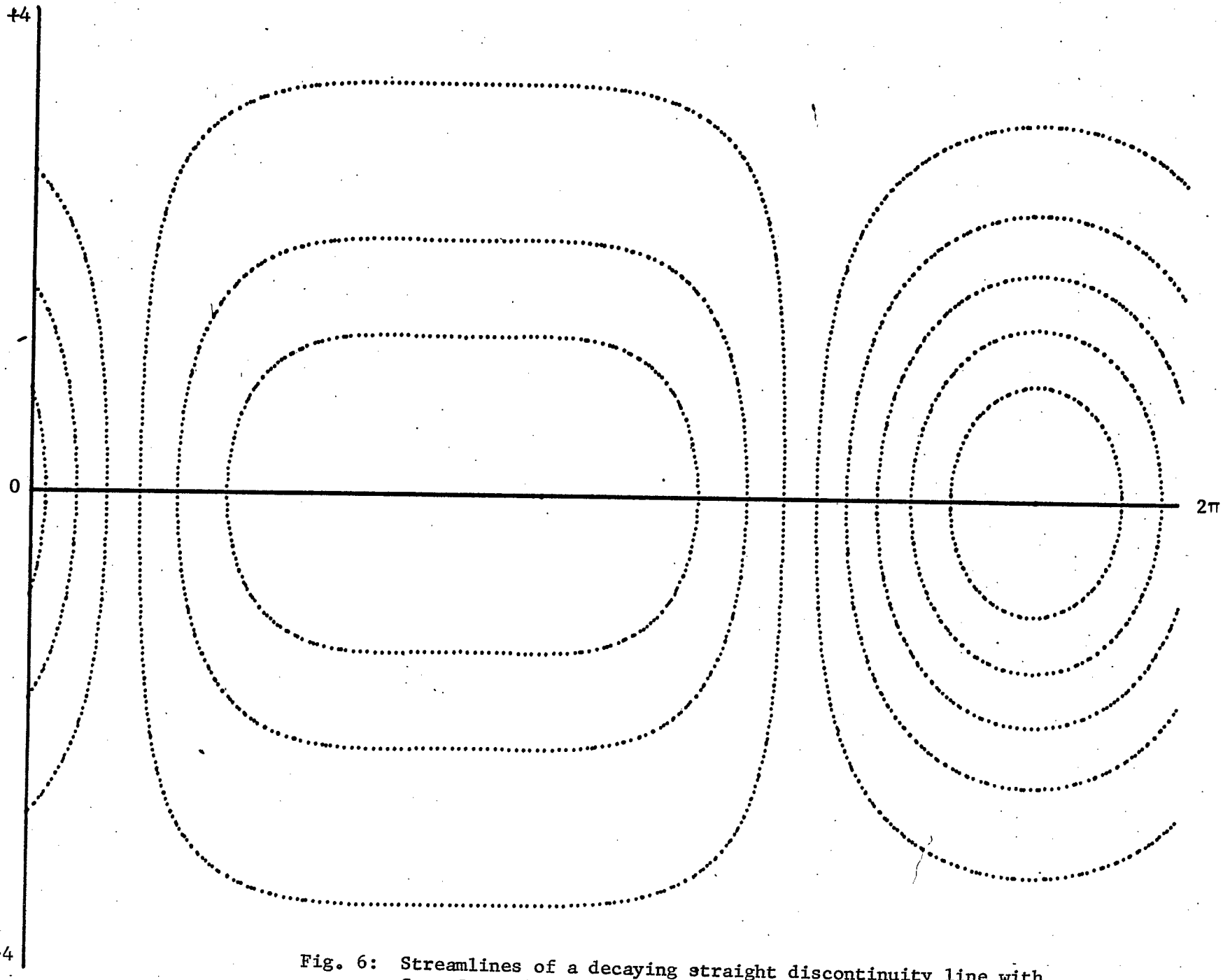

Fig. 6: Streamlines of a decaying straight discontinuity line with $C_2 : C_1 = 10$, $\alpha_2 - \alpha_1 = \pi/4$ at $t = 1.2$.

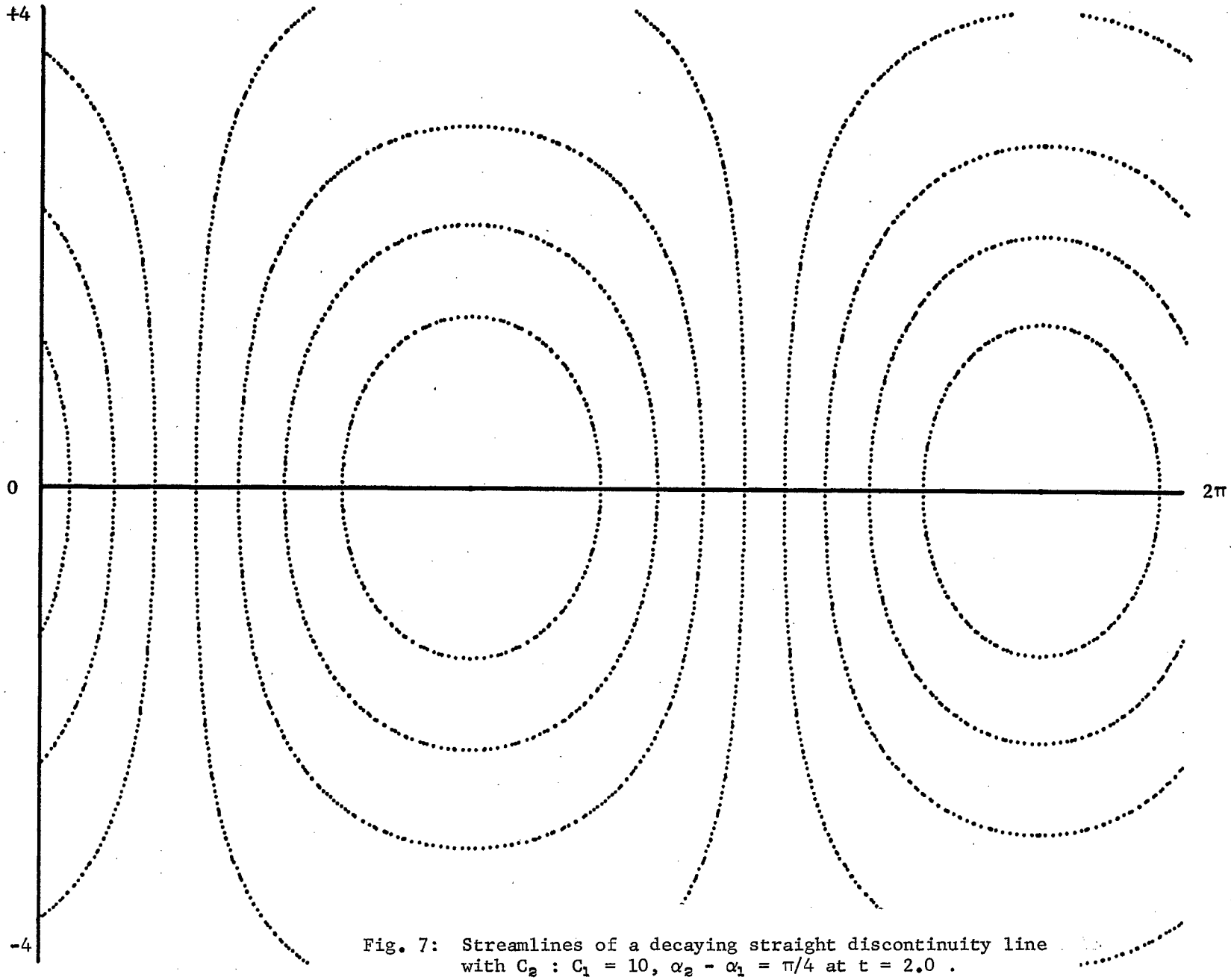

Fig. 7: Streamlines of a decaying straight discontinuity line with $C_2 : C_1 = 10$, $\alpha_2 - \alpha_1 = \pi/4$ at $t = 2.0$.

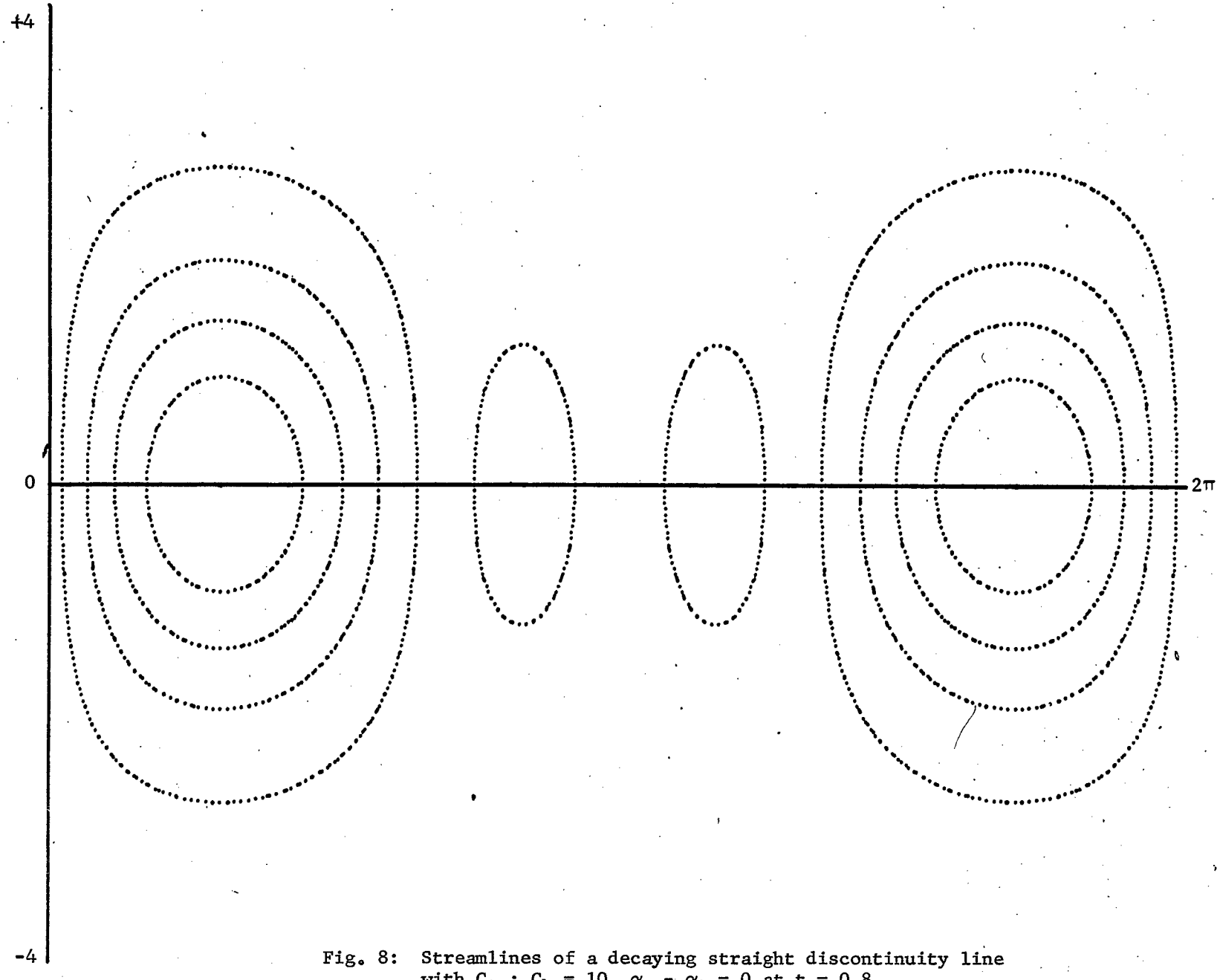

Fig. 8: Streamlines of a decaying straight discontinuity line with $C_2 : C_1 = 10$, $\alpha_2 - \alpha_1 = 0$ at $t = 0.8$.

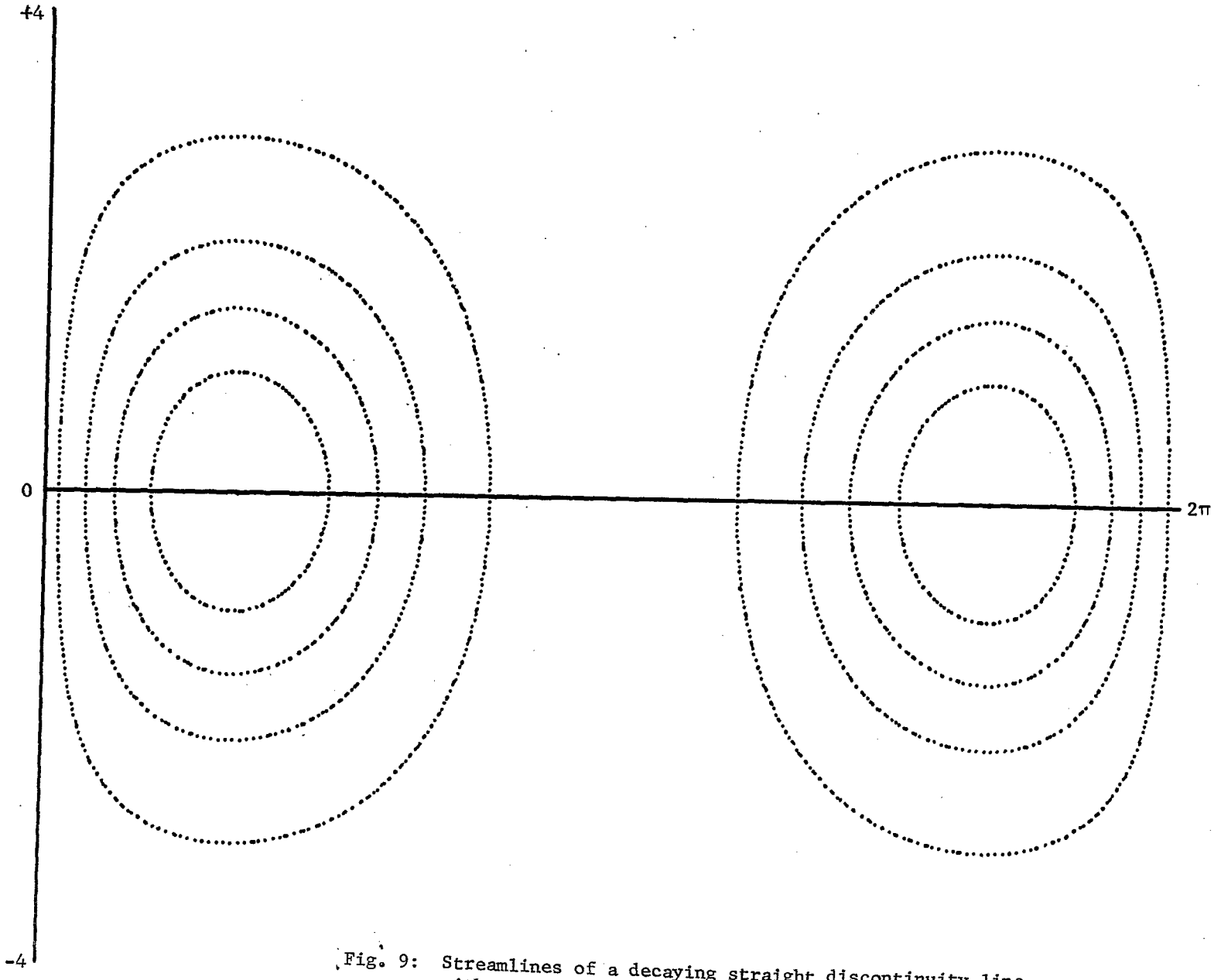

Fig. 9: Streamlines of a decaying straight discontinuity line with $C_2 : C_1 = 10$, $\alpha_2 - \alpha_1 = 0$ at 1.0 .

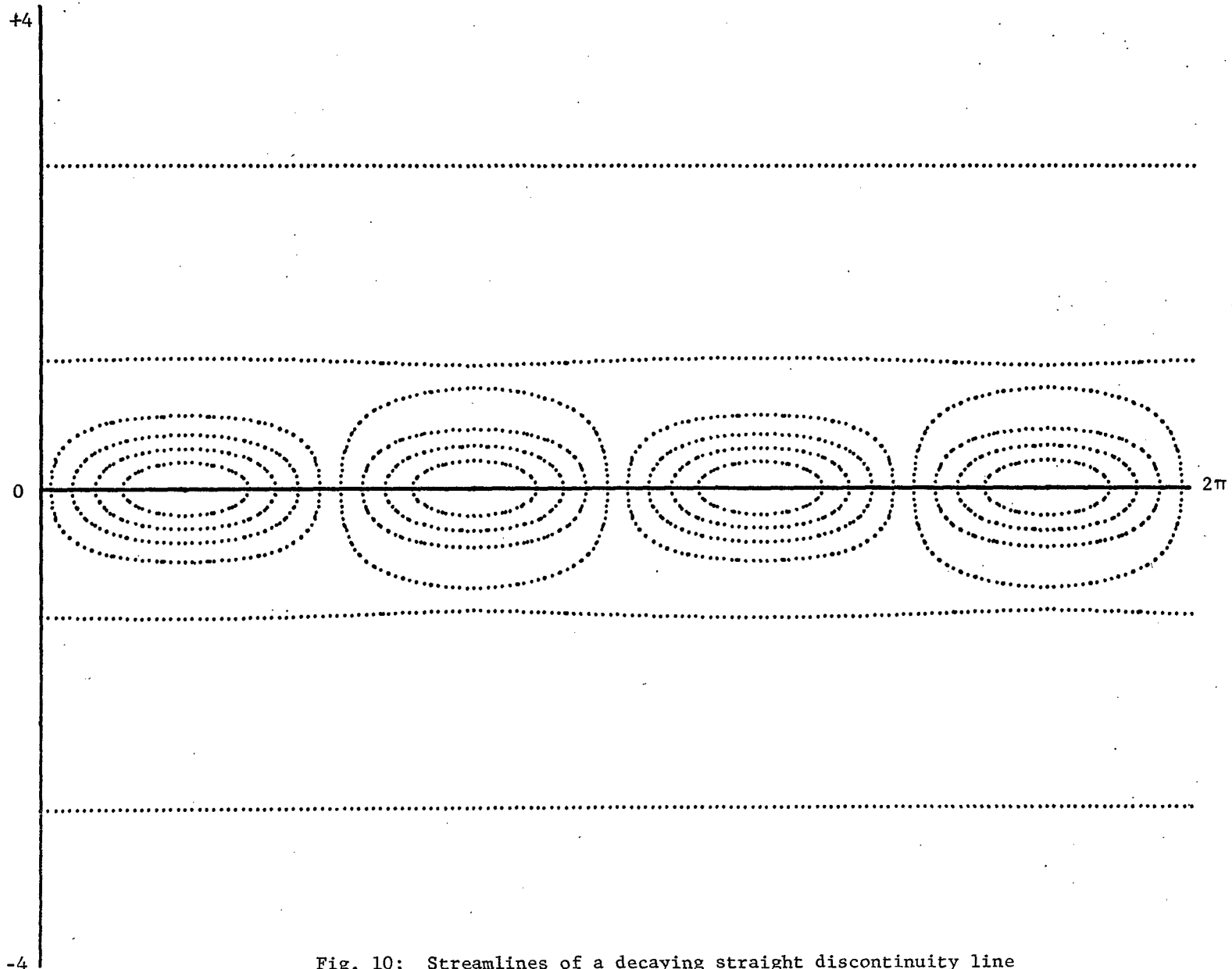

Fig. 10: Streamlines of a decaying straight discontinuity line with C_2 : $A_8 = 5\sqrt{\pi}$, $\alpha_2 = \pi/2$ at t = 0.05 .

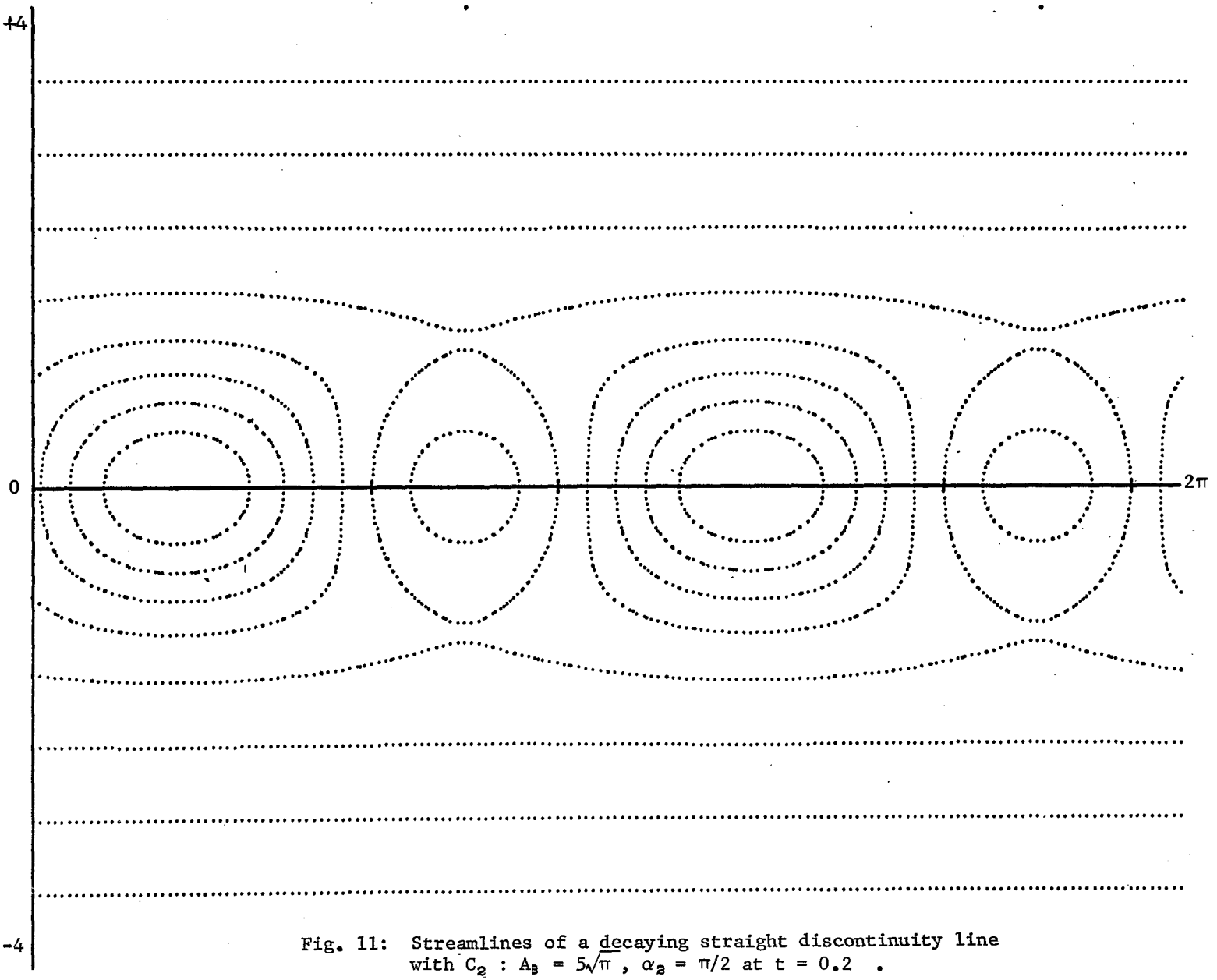

Fig. 11: Streamlines of a decaying straight discontinuity line with C_2 : $A_3 = 5\sqrt{\pi}$, $\alpha_2 = \pi/2$ at $t = 0.2$.

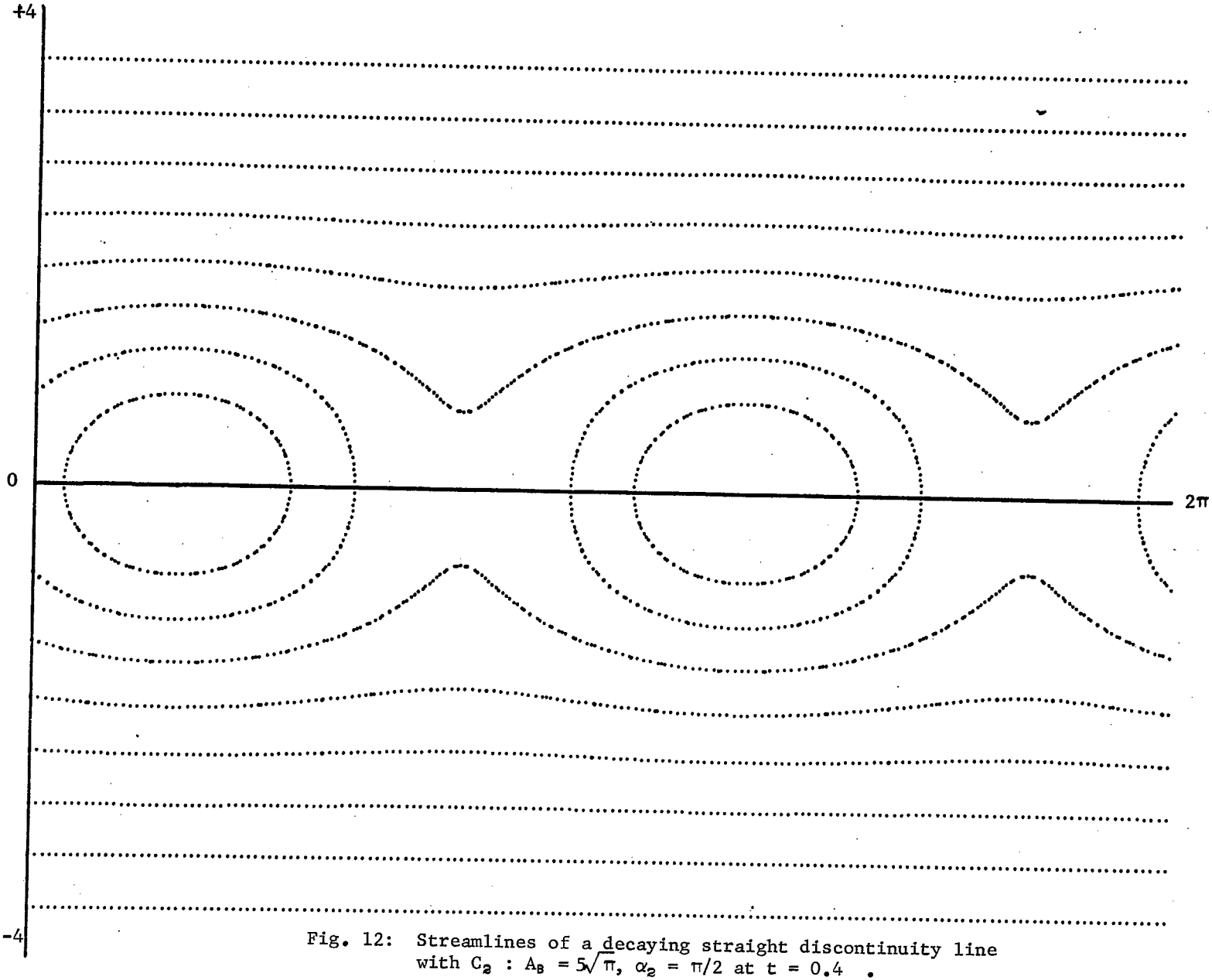

Fig. 12: Streamlines of a decaying straight discontinuity line with C_2 : $A_s = 5\sqrt{\pi}$, $\alpha_2 = \pi/2$ at $t = 0.4$.

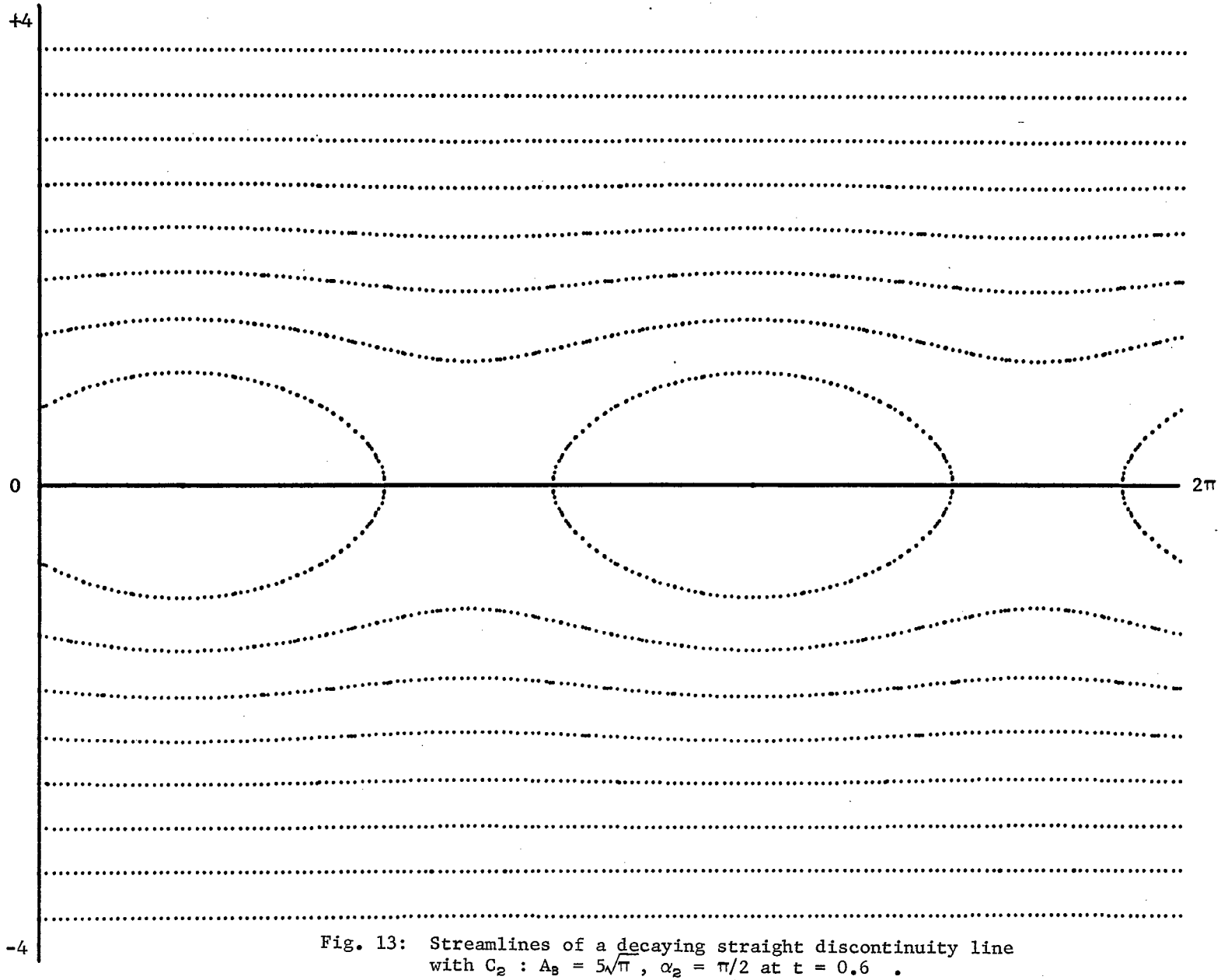

Fig. 13: Streamlines of a decaying straight discontinuity line with C_2 : $A_s = 5\sqrt{\pi}$, $\alpha_2 = \pi/2$ at $t = 0.6$.

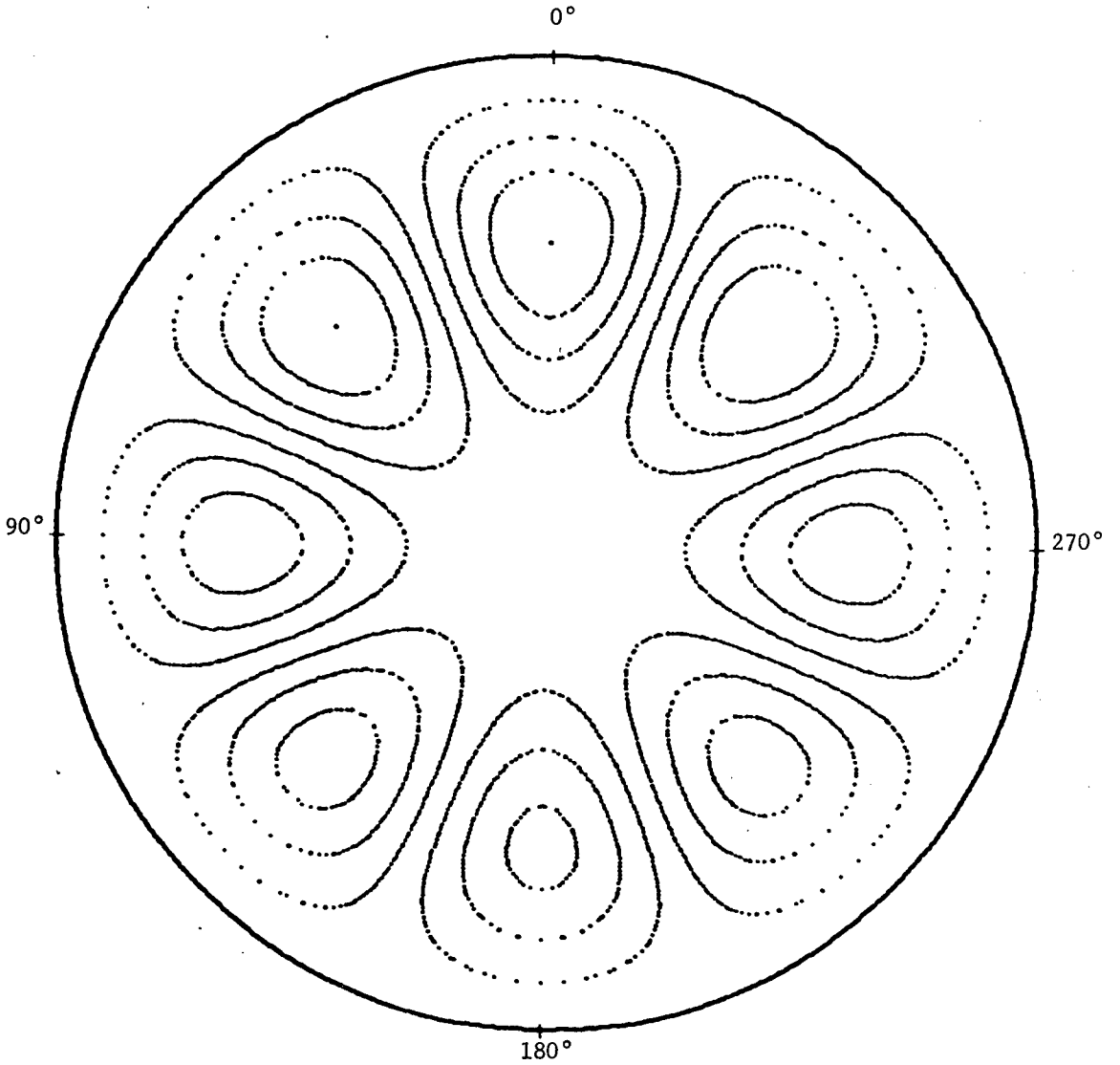

Fig. 14: Streamlines of decaying vortices in a circular region.
$A_4 : A_3 : A_2 = 10{,}000 : 1000 : 1$; $t = 0$.

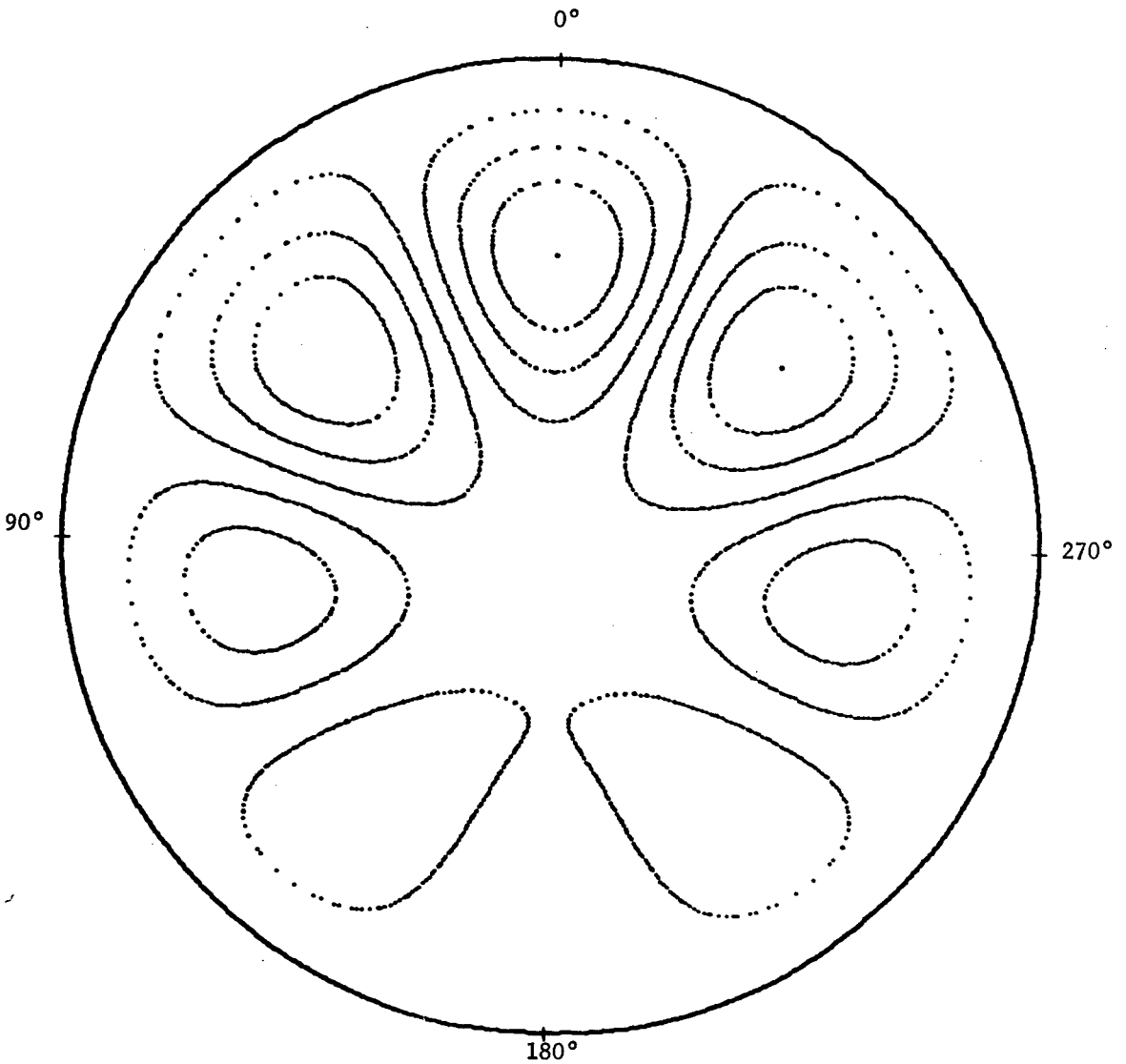

Fig. 15: Streamlines of decaying vortices in a circular region.
$A_4 : A_3 : A_2 = 10{,}000 : 1000 : 1$; $t = 0.11$.

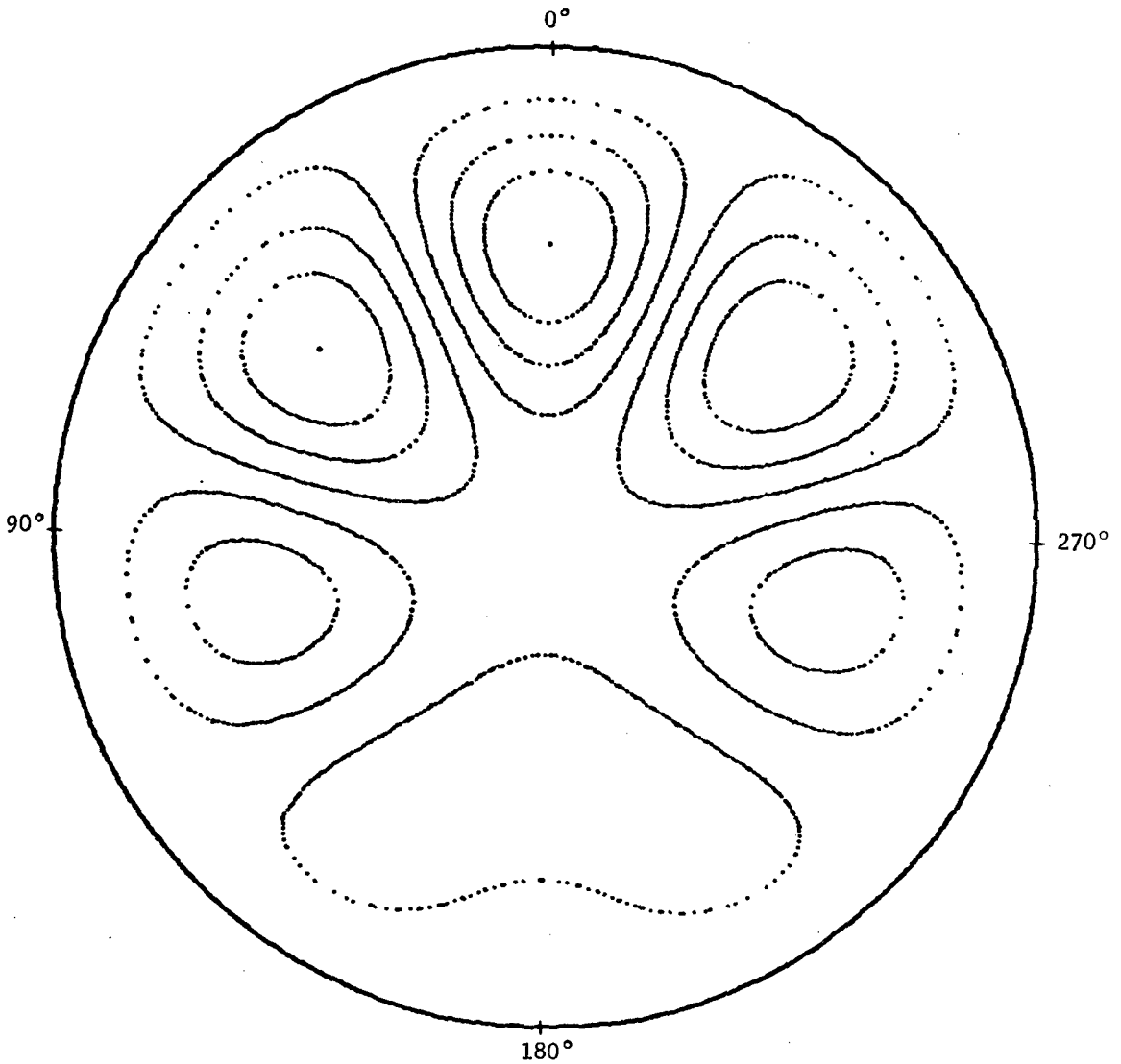

Fig. 16: Streamlines of decaying vortices in a circular region.
$A_4 : A_3 : A_2 = 10{,}000 : 1000 : 1$; $t = 0.13$.

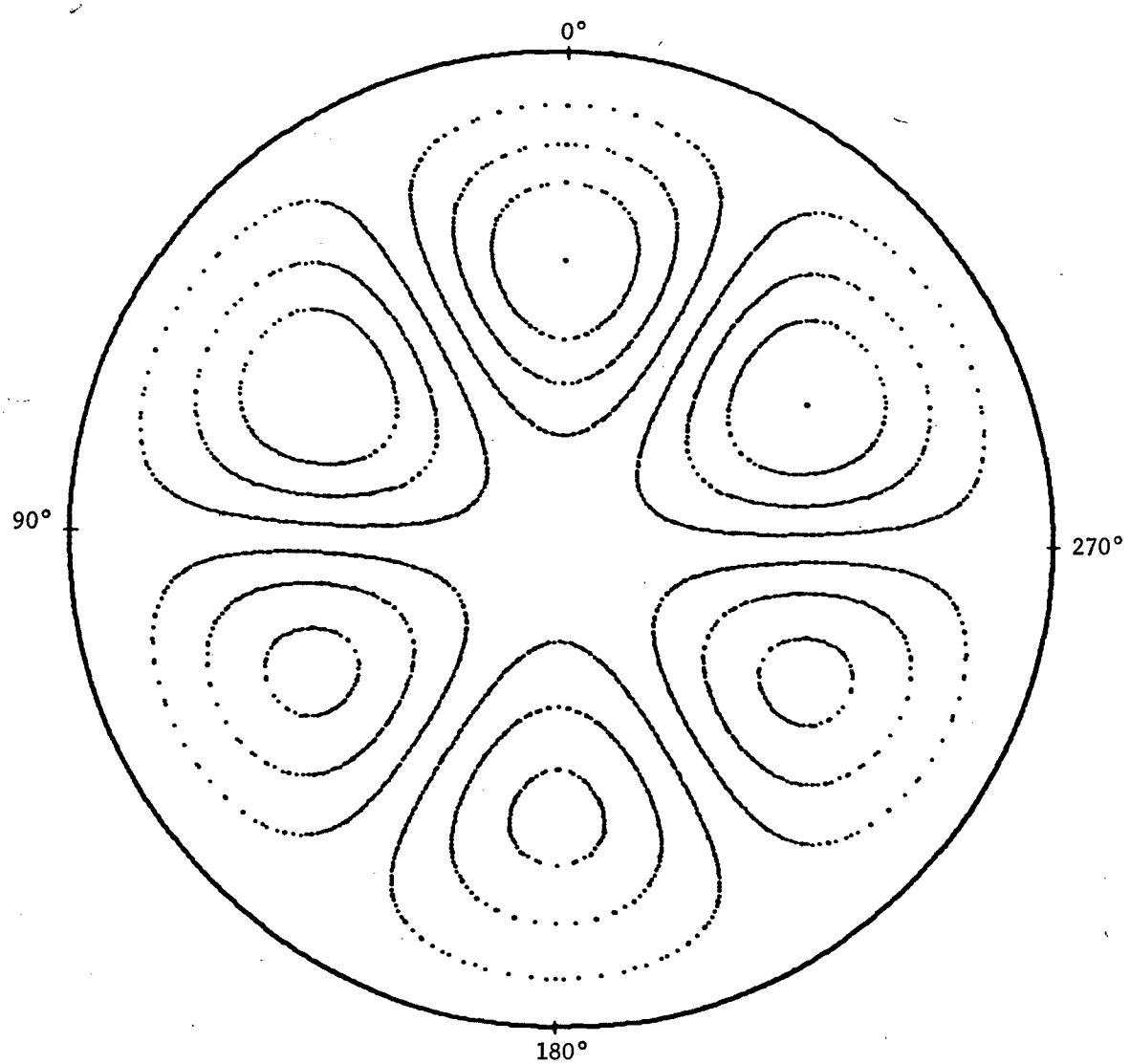

Fig. 17: Streamlines of decaying vortices in a circular region.
$A_4 : A_3 : A_2 = 10{,}000 : 1000 : 1$; $t = 0.25$.

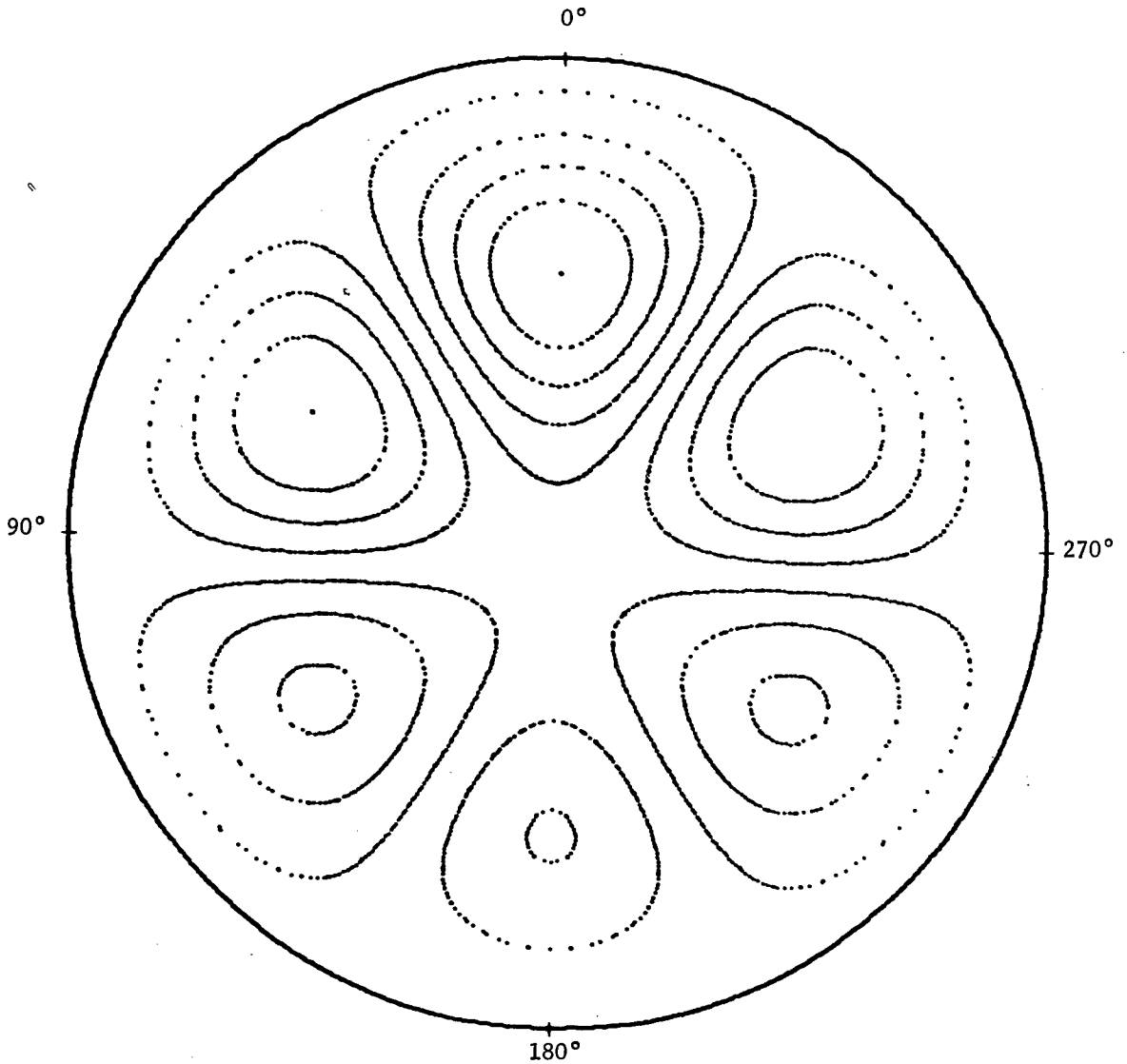

Fig. 18: Streamlines of decaying vortices in a circular region.
$A_4 : A_3 : A_2 = 10{,}000 : 1000 : 1$; $t = 0.35$.

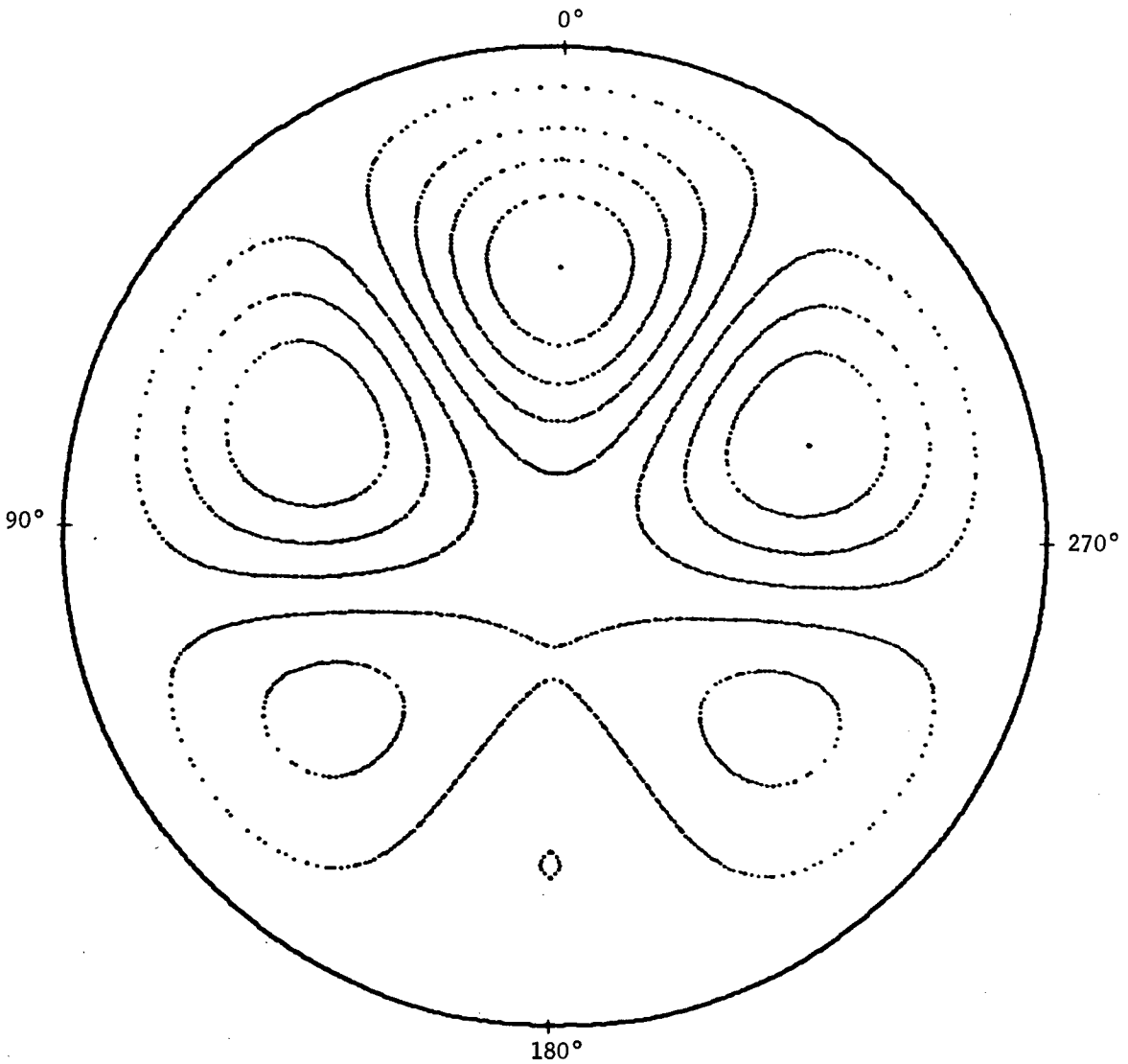

Fig. 19: Streamlines of decaying vortices in a circular region.
$A_4 : A_3 : A_2 = 10{,}000 : 1000 : 1$; $t = 0.39$.

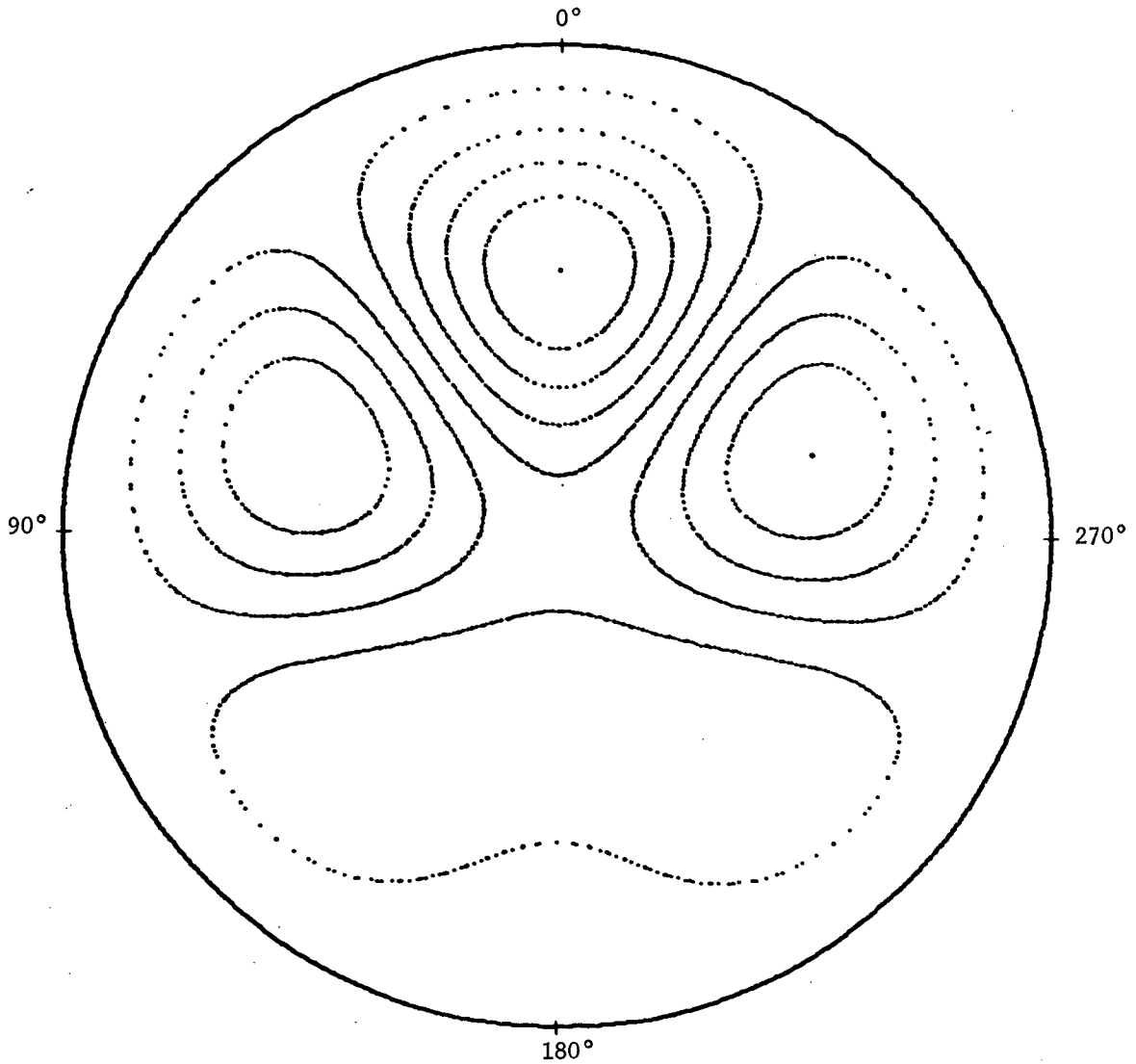

Fig. 20: Streamlines of decaying vortices in a circular region.
$A_4 : A_3 : A_2 = 10{,}000 : 1000 : 1$; $t = 0.42$.

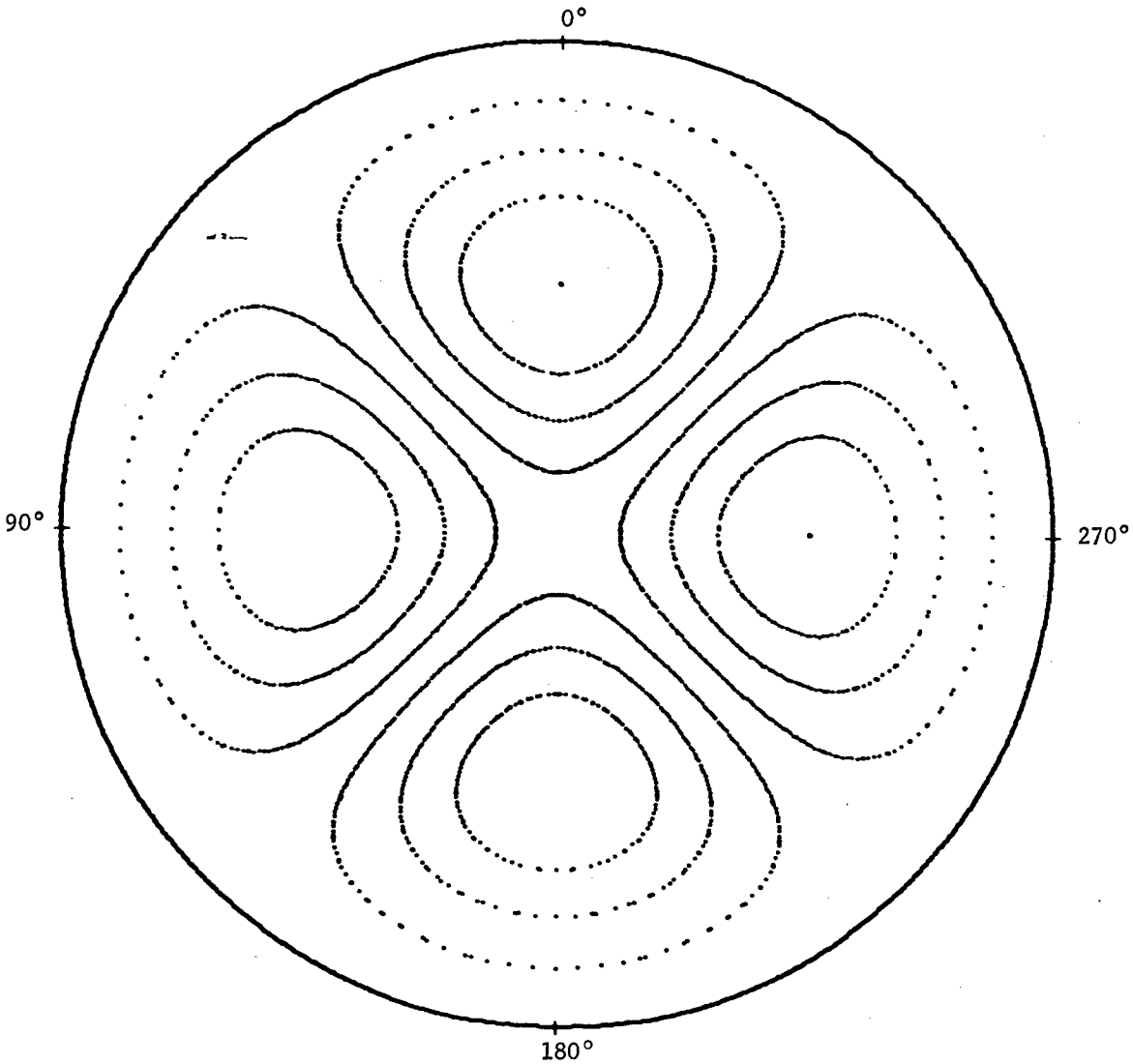

Fig. 21: Streamlines of decaying vortices in a circular region.
$A_4 : A_3 : A_2 = 10{,}000 : 1000 : 1$; $t = 0.8$.

APPENDIX B

DISTRIBUTION

Department of Defense	
Attn: Dr. C. W. Sherwin	1
Department of the Navy	
Office of the Secretary of the Navy	
Attn: Dr. W. P. Raney	1
Department of the Army	
Office of the Secretary of the Army	
Attn: Dr. C. L. Poor	1
Department of the Air Force	
Office of the Secretary of the Air Force	
Attn: Dr. H. Davis	1
Office of the Chief of Naval Operations	
Attn: Mr. A. J. Volta	1
Office of Naval Research	
Attn: Dr. F. J. Weyl	1
Attn: Dr. J. N. Adkins	1
Attn: Dr. S. Silverman	1
Attn: Mrs. D. M. Gilford	1
Attn: Mr. M. Cooper	1
Attn: Mr. R. D. Cooper	1
Attn: Dr. T. L. Saaty	1
Attn: Dr. L. D. Bram	1
Attn: Dr. A. E. Maxwell	1
Attn: Mr. F. D. Jennings	1
Office of the Chief of Research & Development of the Army	
Attn: Dr. H. C. Weber	1
Attn: Dr. R. A. Weiss	1
Air Force Office of Scientific Research	
Attn: Dr. W. J. Price	1
Bureau of Naval Weapons	
Attn: Dr. E. S. Lamar (R-12)	1
Attn: Dr. R. S. Burington (R-14)	1
Attn: Mr. N. E. Promisel (R-15)	1
Attn: Dr. F. I. Tanczos (RM-12)	1
Attn: Mr. J. H. Portch (RR-23)	1
Attn: Mr. S. R. Marcus (RRRE)	1
Attn: Mr. O. Seidman (RRRE-4)	1
Attn: Dr. J. P. Craven (Sp-001)	1
Attn: Mr. W. H. Plant (DLI-3)	2

Bureau of Ships
Attn: Dr. J. H. Huth (3020) 1
Attn: Mr. A. W. Schmidt (3013) 1

Director, Naval Research Laboratory
Washington, D. C. 20390
Attn: Dr. R. M. Page 1
Attn: Technical Library 1

Commander, Naval Ordnance Laboratory
White Oak, Maryland
Attn: Dr. R. E. Wilson 1
Attn: Dr. D. F. Bleil 1
Attn: Dr. R. C. Roberts 1
Attn: Dr. K. R. Enkenhus 1
Attn: Technical Library 1

Director, David Taylor Model Basin
Washington, D. C. 20007
Attn: Dr. A. H. Keil 1
Attn: Mr. G. H. Gleissner 1
Attn: Dr. W. E. Cummins 1
Attn: Dr. H. R. Chaplin 1
Attn: Dr. F. H. Todd 1
Attn: Dr. F. N. Frenkiel 1
Attn: Mr. R. M. Stevens 1
Attn: Dr. S. de los Santos 1
Attn: Dr. A. Borden 1
Attn: Mrs. J. W. Schot 1
Attn: Mr. C. W. Dawson 1
Attn: Technical Library 1

Commander, Naval Ordnance Test Station
China Lake, California
Attn: Dr. W. R. Haseltine 1
Attn: Dr. D. E. Zilmer 1
Attn: Technical Library 1

Commander, Naval Ordnance Test Station
Pasadena Annex, California
Attn: Dr. J. W. Hoyt 1
Attn: Dr. J. G. Waugh 1
Attn: Technical Library 1

Commander, Naval Electronics Laboratory
San Diego, California
Attn: Technical Library 1

Superintendent, Naval Postgraduate School
Monterey, California
Attn: Library, Technical Reports Section 1

Superintendent, Naval Academy
Annapolis, Maryland
Attn: Department of Mathematics 1
Attn: Technical Library 1

U. S. Army Mathematics Research Center
University of Wisconsin
Madison 6, Wisconsin
Attn: Dr. P. C. Jain 1
Attn: Dr. R. Manohaw 1
Attn: Technical Library 1

Commanding Officer, U S. Army Research Office - Durham
Durham, North Carolina 27706
Attn: CRD-AA-IPL, Box CM 1

Commanding General, White Sands Proving Ground
Las Cruces, New Mexico
Attn: Flight Determination Laboratory 1

Commanding General, Aberdeen Proving Ground
Aberdeen, Maryland
Attn: Technical Library 1

Mr. A. Flatau
Army Chemical Center
Edgewood Arsenal, Maryland 1

Wright-Patterson Air Force Base, Ohio 45433
Attn: RTD-SEPIR 1

Defense Documentation Center
Cameron Station
Alexandria, Virginia 20

National Aeronautics and Space Administration
Washington, D. C.
Attn: Technical Library 2

National Aeronautics and Space Administration
Goddard Space Flight Center
Greenbelt, Maryland
Attn: Mr. A. B. Riley 1
Attn: Technical Library 1

National Aeronautics and Space Administration
Marshall Space Flight Center
Huntsville, Alabama
Attn: Technical Library 1

National Aeronautics and Space Administration
Lewis Research Center
Cleveland 35, Ohio
Attn: Technical Library 1

National Aeronautics and Space Administration
Ames Research Center
Moffett Field, California
Attn: Dr. E. D. Martin 1
Attn: Technical Library 1

U. S. Atomic Energy Commission
Washington, D. C.
Attn: Technical Library 1

Oak Ridge National Laboratory
Oak Ridge, Tennessee
Attn: Dr. J. J. Keyes, Jr. 1
Attn: Technical Library 1

Director, National Bureau of Standards
Washington, D. C. 20234
Attn: Technical Library 1

U. S. Weather Bureau
Washington, D. C. 20235
Attn: Dr. J. Smagorinsky 1
Attn: Dr. L. Rintel 1
Attn: Dr. K. Bryan 1
Attn: Dr. L. P. Harrison (EFFA) 1
Attn: Technical Library 1

National Science Foundation
1520 H Street, N. W.
Washington, D. C.
Attn: Mathematical Sciences Division 1
Attn: Engineering Sciences Division 1

Prof. J. G. Charney
Massachusetts Institute of Technology
Cambridge, Massachusetts 1

University of Maryland
College Park, Maryland
Attn: Prof. J. Weske 1
Attn: Inst. for Fluid Dynamics and Appl. Mathematics 1

Stanford University
Stanford, California
Attn: Prof. M. Van Dyke 1
Attn: Prof. Flügge-Lotz 1

University of California
Berkeley 4, California
Attn: Prof. Chang-Lin Tien 1
Attn: Department of Mathematics 1

Los Alamos Scientific Laboratory
Los Alamos, New Mexico
Attn: Dr. J. E. Fromm 1
Attn: Technical Library 1

Applied Physics Laboratory
The Johns Hopkins University
Silver Spring, Maryland
Attn: Technical Library 1

Prof. J. D. Nicolaides
University of Notre Dame
Notre Dame, Indiana 46556 1

Prof. W. Squire
West Virginia University
Morgantown, W. Va. 1

Prof. M. Z. v. Krzywoblocki
Michigan State University
East Lansing, Michigan 1

Prof. T. Ranov
State University of New York
Buffalo 14, New York 1

Prof. Simon Ostrach
Case Institute of Technology
Cleveland 6, Ohio 1

Mathematics Department
American University
Washington, D. C. 1

Mathematics Department
George Washington University
Washington, D. C. 1

University of Chicago
Chicago, Illinois
Attn: Prof. D. Fultz 1
Attn: Prof. H. L. Kuo 1

Woods Hole Oceanographic Institute
Woods Hole, Massachusetts
Attn: Technical Library 1

Dr. C. C. Bramble
145 Monticello
Annapolis, Maryland 1

Dr. R. H. Lyddane
General Electric Company
1 River Road
Schenectady, New York 1

Dr. W. E. Langlois
IBM Research Laboratory
San Jose, California 1

Prof. Ian S. Gartshore
McGill University
Montreal, Quebec, Canada 1

Mr. D. F. van der Merwe
Pulp and Paper Research Institute of Canada
Montreal 2, Canada 1

Prof. N. Riley
University of East Anglia
Norwich, England 1

Prof. K. Stewartson
Dept. of Mathematics
University College
London, England 1

Local:
D 1
K 1
K-1 1
K-3 1
KXK 1
KXH 1
KYS 50
MAL 6
File 1

UNCLASSIFIED

Security Classification

DOCUMENT CONTROL DATA - R&D

(Security classification of title, body of abstract and indexing annotation must be entered when the overall report is classified)

1. ORIGINATING ACTIVITY *(Corporate author)*	2a. REPORT SECURITY CLASSIFICATION
Naval Weapons Laboratory	UNCLASSIFIED
	2b. GROUP

3. REPORT TITLE

DECAY OF A DISCONTINUITY LINE IN A VISCOUS FLUID

4. DESCRIPTIVE NOTES *(Type of report and inclusive dates)*

5. AUTHOR(S) *(Last name, first name, initial)*

Lugt, Hans J.

6. REPORT DATE	7a. TOTAL NO. OF PAGES	7b. NO. OF REFS
May 1966	48	

8a. CONTRACT OR GRANT NO.	9a. ORIGINATOR'S REPORT NUMBER(S)
b. PROJECT NO.	2038
c.	9b. OTHER REPORT NO(S) *(Any other numbers that may be assigned this report)*
d.	

10. AVAILABILITY/LIMITATION NOTICES

Distribution of this document is unlimited.

11. SUPPLEMENTARY NOTES	12. SPONSORING MILITARY ACTIVITY

13. ABSTRACT

Integral transforms are used to solve singular initial value problems for Stokes' slow-motion equations. The method is applied to investigate the decaying process of straight and circular discontinuity lines as well as the dissipation of local disturbances in an infinite medium. A criterion for the occurrence of secondary vortices is derived. Numerical results are displayed for periodic initial disturbances which demonstrate graphically the spreading of the disturbance from a discontinuity line into the fluid under successive development and decay of secondary vortices. A more detailed sequence of dissipating vortices is evaluated numerically and displayed by streamline patterns in connection with Lamb's vortical eigenmotions in an infinitely long cylinder of finite radius.

DD FORM 1 JAN 64 1473

UNCLASSIFIED

Security Classification

Naval Weapons Laboratory. (NWL Technical Report 2038) DECAY OF A DISCONTINUITY LINE IN A VISCOUS FLUID, by Hans J. Lugt. May 1966. 20 pages, 21 figures. UNCLASSIFIED REPORT	1. Fluids - Viscosity 2. Fluids - Mathematical analysis I. Lugt, Hans J. UNCLASSIFIED CARD	Naval Weapons Laboratory. (NWL Technical Report 2038) DECAY OF A DISCONTINUITY LINE IN A VISCOUS FLUID, by Hans J. Lugt. May 1966. 20 pages, 21 figures. UNCLASSIFIED REPORT	1. Fluids - Viscosity 2. Fluids - Mathematical analysis I. Lugt, Hans J. UNCLASSIFIED CARD
Naval Weapons Laboratory. (NWL Technical Report 2038) DECAY OF A DISCONTINUITY LINE IN A VISCOUS FLUID, by Hans J. Lugt. May 1966. 20 pages, 21 figures. UNCLASSIFIED REPORT	1. Fluids - Viscosity 2. Fluids - Mathematical analysis I. Lugt, Hans J. UNCLASSIFIED CARD	Naval Weapons Laboratory. (NWL Technical Report 2038) DECAY OF A DISCONTINUITY LINE IN A VISCOUS FLUID, by Hans J. Lugt. May 1966. 20 pages, 21 figures. UNCLASSIFIED REPORT	1. Fluids - Viscosity 2. Fluids - Mathematical analysis I. Lugt, Hans J. UNCLASSIFIED CARD